

# Analysis of CIZ1 Variant Expression in Breast Cancer Cells

Ernesto López de Alba (MSc)

Master of Science by Research

University of York

Biology

February 2020

## Abstract

---

CIZ1 is a nuclear matrix (NM) protein, which helps to coordinate the recruitment of cyclins E and A during initiation of DNA replication in mammalian cells. CIZ1 contains two characterised functional domains: anchor domain (AD) supports attachment to the NM, whilst the replication domain (RD) supports direct interaction with cyclins. Recent publications implicate CIZ1 in coupling DNA replication with maintenance of repressive secondary modifications of histone proteins that specify epigenetic state. CIZ1 aberrant expression has been extensively linked with cancer, mostly at the level of alternative splicing, and we have transcript-level evidence that CIZ1 RD and AD are expressed differently in common solid tumours. My project explores these observations and extends them to the protein level. I show that CIZ1 accumulation at the inactive X chromosome seen in primary epithelial breast cells, is compromised in breast cancer cells. I present evidence of uncoupled CIZ1 domain expression and high diversity of CIZ1 species in normal and cancer breast cells, and show that CIZ1 expression variability occurs mostly at protein level. My data also begins to suggest the existence of cancer-specific CIZ1 fragments presenting altered aggregation states. I also present evidence that implicates CIZ1-RD polyQ regions as a dominant-negative force acting upon endogenous CIZ1 assemblies. Overall, the emerging picture is complex and my analysis suggests several new lines of investigation.

# Table of Contents

---

ABSTRACT .....	2
TABLE OF CONTENTS.....	3
LIST OF FIGURES.....	5
LIST OF TABLES .....	6
ACKNOWLEDGEMENTS .....	7
AUTHOR'S DECLARATION .....	8
CHAPTER 1: INTRODUCTION .....	9
1.    DISCOVERY OF CIZ1 AND ITS ROLE IN THE REGULATION OF DNA REPLICATION.....	9
2.    CIZ1 REGULATES THE G1/S TRANSITION OF MAMMALIAN CELLS. ....	9
3.    MRNA AND PROTEIN DOMAIN ARCHITECTURE OF CIZ1. ....	11
4.    CIZ1 FACILITATES XIST LOCALIZATION TO THE INACTIVE X-CHROMOSOME.....	12
5.    CIZ1 ABERRANT EXPRESSION AND CANCER. ....	13
6.    CIZ1, XI EPIGENETIC INSTABILITY AND BREAST CANCER. ....	14
7.    HYPOTHESIS AND AIMS. ....	15
CHAPTER 2. MATERIALS AND METHODS .....	16
1.    CELL CULTURE. ....	16
1.1.    HUMAN CELL LINES USED. ....	16
1.2.    PRIMARY CELLS. ....	16
2.    MAINTENANCE.....	16
3.    IMMUNOFLUORESCENCE. ....	17
3.1.    NUCLEAR MATRIX EXTRACTION. ....	18
3.2.    PLASMID DNA TRANSFECTION.....	18
3.3.    IMAGING. ....	19
3.4.    STATISTICAL ANALYSIS. ....	19
4.    RNA ANALYSIS.....	19
4.1.    TOTAL RNA EXTRACTION.....	19
4.2.    REVERSE TRANSCRIPTION QUANTITATIVE PCR (RT-qPCR). ....	20
4.3.    NORTHERN BLOTTING.....	20
4.4.    PRIMERS AND PROBES.....	21
5.    PROTEIN ANALYSIS. ....	22
5.1.    TOTAL PROTEIN LYSATES FORM CELLS. ....	22
5.2.    SDS-PAGE GELS AND TRANSFER.....	22
5.3.    WESTERN BLOTTING. ....	22
5.4.    IMMUNOPRECIPITATION .....	23
5.5.    ANTIBODIES. ....	23
CHAPTER 3. IMMUNOFLUORESCENCE ANALYSIS OF CIZ1 EXPRESSION IN BREAST CANCER .....	25
1.    INTRODUCTION.....	25
2.    AIMS. ....	26
3.    EXPERIMENTAL DESIGN. ....	26
4.    RESULTS.....	26
4.1.    SELECTED CELLS AND CELL LINES REPRESENT THE MOLECULAR SUBTYPES OF BREAST CANCER, THE CULTURE-ADAPTED NON-CANCEROUS STATE AND THE <i>BASAL STATE</i> OF THE HUMAN FEMALE BREAST TISSUE. ....	26
4.2.    CIZ1 ACCUMULATES AT THE XI AND MIGHT BE IMPLICATED IN XI RELOCATION DURING S-PHASE IN HPMECS.	

4.3.	CIZ1 DOMAINS COLOCALISE IN FOCI IN ALL HPMECS BUT ONLY IN SOME 1-7HB2 AND MCF10A CELLS. ....	31
4.4.	CIZ1 FOCI DISRUPTION AND LACK OF CIZ1 DOMAIN COLOCALISATION IN CANCER CELL LINES.....	31
5.	CONCLUSIONS. ....	34
<b>CHAPTER 4. CIZ1 EXPRESSION ANALYSIS IN BREAST CANCER: RNA LEVEL .....</b>		<b>35</b>
1.	INTRODUCTION.....	35
2.	AIMS . ....	36
3.	EXPERIMENTAL DESIGN. ....	36
4.	RESULTS.....	37
4.1.	CIZ1 EXPRESSION IS DOMAIN-BALANCED IN ALL CELL TYPES AND OVERREPRESENTED IN EARLY STAGES OF BREAST CANCER. ....	37
4.1.1.	TECHNICAL CONSIDERATIONS. ....	38
4.2.	NO EVIDENCE OF ALTERNATIVE TRANSCRIPTS.....	39
5.	CONCLUSIONS. ....	41
<b>CHAPTER 5: ANALYSIS OF CIZ1 EXPRESSION IN BREAST CANCER: PROTEIN LEVEL.....</b>		<b>42</b>
1.	INTRODUCTION.....	42
2.	AIMS. ....	43
3.	EXPERIMENTAL DESIGN. ....	43
4.	RESULTS.....	43
4.1.	HIGH DIVERSITY OF CIZ1 SPECIES AND DOMAIN-SPECIFIC FRAGMENTS IN NORMAL AND CANCER CELLS.....	43
4.2.	CANCER-SPECIFIC CIZ1 FRAGMENTS INTERACT WITH THE NUCLEAR MATRIX IN AN RNA-INDEPENDENT FASHION. 46	46
4.3.	CIZ1-F IS NOT EXPRESSED IN HPMECS AND AFFECTS ENDOGENOUS CIZ1 AGGREGATION IN 1-7HB2 CELLS..	49
5.	CONCLUSIONS. ....	52
<b>CHAPTER 6: DISCUSSION .....</b>		<b>53</b>
<b>APPENDIX .....</b>		<b>57</b>
1.	CIZ1 IMPLICATION IN HUMAN PATHOLOGY: BIBLIOGRAPHIC SUMMARY.....	57
2.	NEGATIVE CONTROL OF SERIAL NUCLEAR EXTRACTION. ....	60
3.	ANTIBODY VALIDATION. ....	61
<b>REFERENCES.....</b>		<b>63</b>

## List of Figures

---

### CHAPTER 1

Figure 1.1 Replication complex assembly from origin specification to replisome formation.....10

Figure 1.2 mRNA and protein domain architecture of CIZ1 .....11-12

### CHAPTER 3

Figure 3.1 Current subtyping schemes of breast cancer cell lines and cells used in this study ...  
.....27-28

Figure 3.2 CIZ1 colocalises with the Xi markers and presents a predominantly peripheral position in the nucleus of HPMECs and 1-7 HB2 cells .....30

Figure 3.3 CIZ1 domains colocalise in foci in all HPMECs but only in some 1-7 HB2 and MCF10A cells.....32

Figure 3.4 CIZ1 location is highly altered in breast cancer cells cancer .....33-34

### CHAPTER 4

Figure 4.1 Imbalanced CIZ1 domain expression in common solid tumours .....35-36

Figure 4.2 CIZ1 domain expression is imbalanced is expressed and upregulated in early staged of the tumour .....37-38

Figure 4.3 CIZ1 domain expression levels internally normalised to the expression level of a population (Primary 1) of HPMECs using the formula  $2^{-\Delta\Delta Ct}$  .....39

Figure 4.4 CIZ1 is expressed as a single transcript containing both CIZ1 functional domains .....  
.....40

### CHAPTER 5

Figure 5.1 CIZ1 protein expression is highly complex and exhibit normal/cancer patterns .....45

Figure 5.2 Serial matrix extractions revealed aberrant CIZ1 extractability profiles in cancer cells  
.....47-49

Figure 5.3 CIZ1-F is variably expressed by breast cell lines but not HPMECs .....50

Figure 5.4 CIZ1-F and N-57 significantly affect endogenous CIZ1 capacity to aggregate .....51-52

### APPENDIX

Figure A.1 Negative control of serial nuclear extraction .....60

Figure A.2 Immunofluorescence-Western blot antibody validation .....62

## List of Tables

---

### CHAPTER 1

Table 1 CIZ1 is associated with tumour growth in multiple cancers .....	13
---	----

### CHAPTER 2

Table 2.1 Cell line information .....	15
Table 2.2 Details of cell culture media for cell lines used .....	17
Table 2.3 CIZ1 transfection constructs .....	18
Table 2.4 Primers for qPCR and probe design .....	21
Table 2.5 Probes for Northern blot analysis .....	21
Table 2.6 Details of antibodies used, buffers and incubation times .....	23-24
Table 2.7 Anti-CIZ1 antibodies, sources, antigens and known behaviours .....	24

### APPENDIX

Table A.1 Exhaustive summary of studies implicating CIZ1 in human disease .....	57-59
---	-------

## Acknowledgements

---

This research was carried out with the support of the University of York, which partially funded the costs of this study. I would like to thank Breast Cancer Now and the anonymous donors of normal human breast tissue, for kindly providing the primary breast epithelial cells utilised in this research. I also wanted to express my gratitude to Dr Sajad Sofi for his technical support for the RNA work and valuable scientific advice.

I would like to express special gratitude to my supervisor Prof. Dawn Coverley, who gifted me with the opportunity to access high-level research, and whose patience, attentiveness and dedication represented a precedent that nourish my passion for science. I also wanted to thank Dr Justin Ainscough for his technical guidance and insightful discussions. The benefits of my enjoyable experience in Coverley lab extend far beyond the scientific aspect, for which I wanted to thank all its members, and my colleagues of the University of York.

Most importantly, I would like to thank my mother for her indispensable love and support.

## Author's Declaration

---

I declare that this thesis is a presentation of original work and I am the sole author, with the following exceptions:

### **CHAPTER 5:**

GFP-CIZ1 mouse construct N57 was kindly provided by the undergraduate student Susie Holliman (Coverley lab). Human GFP-CIZ1-F construct was kindly provided by Dr Dorian Swarts (Coverley Lab).

This work has not previously been presented for an award at this, or any other, University. All sources are acknowledged as References.

## Chapter 1: Introduction

---

### 1. Discovery of CIZ1 and its role in the regulation of DNA replication.

The correct replication of DNA is a fundamental requisite for any given cell prior to its segregation and division into two daughter cells. Exact duplication of the genome, and associated proteins and RNAs is linked to the long-term homeostasis of pluricellular organisms. Chromatin replication presents multiple layers of regulation that are highly orchestrated to ensure its occurrence once and only once per cell cycle while achieving a level of precision with an error rate at less than 1 per billion bases copied <sup>1</sup>. This is accomplished by the concerted activity of a family of proteins called cyclin-dependent kinases (CDKs), which phosphorylate key targets to promote DNA synthesis and mitotic progression <sup>2</sup>. CDKs remain inactive until bound by cyclin subunits, which are specifically expressed at certain points of the cell cycle thanks to a tightly regulated synthesis and ubiquitin-dependent proteolysis <sup>2</sup>. Cyclin-binding allows inactive CDKs to adopt an active configuration while providing temporal regulation and target specificity. On top of this, a second layer of regulation consists in the activity of small inhibitory proteins, the CKIs, which serve as brakes to halt cell cycle progression under unfavourable conditions by blocking phosphate transfer to the substrate in a process known as the cell cycle checkpoint <sup>3</sup>. For this reason, proteins that directly interact with cyclins, CDKs and CKIs are of central importance in the understanding of the cell cycle regulation.

The main checkpoint of DNA replication is the DNA damage checkpoint, where the tumour suppressor p53 can mediate either growth arrest or apoptosis in response to DNA breakage <sup>4</sup>. To search for binding partners of the p53 direct target CKI p21<sup>Cip1</sup> that could regulate its subcellular compartmentalisation and degradation, a yeast two-hybrid screening was performed using cyclin E- p21<sup>Cip1</sup> as a bait. This led to the identification of the protein later named CDKN1A-Interacting Zinc Finger Protein 1 (CIZ1) <sup>5,6</sup>.

### 2. CIZ1 regulates the G1/S transition of mammalian cells.

Further research would reveal that CIZ1 is a nuclear matrix (NM) protein with homologues in human, mouse and other vertebrates, that promotes initiation of mammalian DNA replication <sup>7,8</sup>. One of the main regulation points of DNA replication is the initiation of DNA synthesis, which occurs in late G1 phase and allows the cell cycle progression from G1 to the S phase <sup>9</sup>. DNA

replication requires two main groups of initiating proteins. First, the origin recognition complex (ORC) composed of ORC1-6 is assembled in G1 phase. The ORC recognises and binds multiple sites in the DNA where the DNA replication will initiate. To form the pre-replication complex (pre-RC), the ORC complex recruits cell division cycle 6 (CDC6), chromatin licensing and DNA replication factor 1 (CDT1), which loads a hexamer of minichromosome maintenance proteins (MCM2-7) and completes replication licensing at the associated origin<sup>10-12</sup>

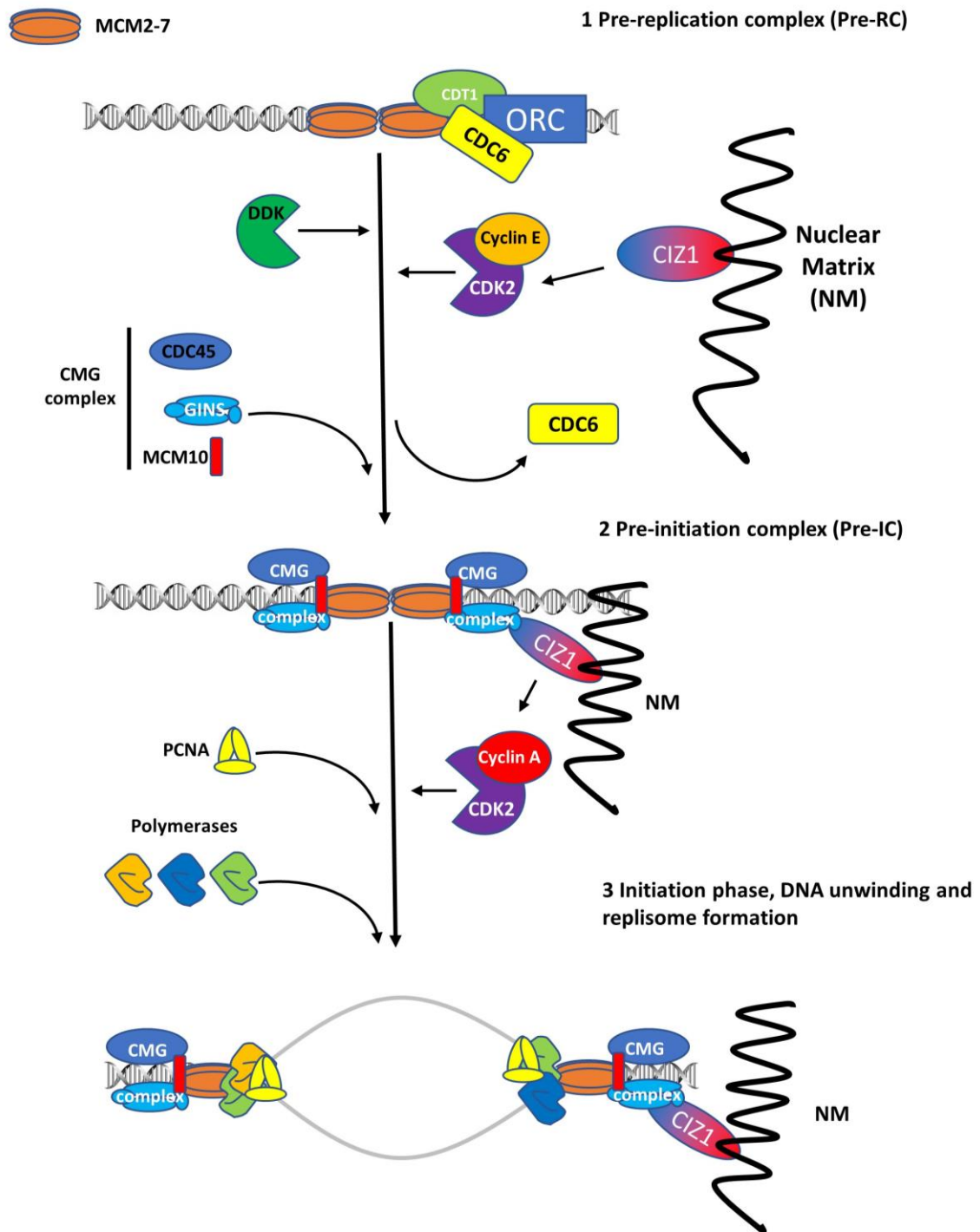


Figure 1.1 Replication complex assembly from origin specification to replisome formation<sup>13</sup>.

This complex process is conserved in eukaryotes <sup>14</sup> and once the cells enter late-G1phase, putative replication origins are activated by a second group of proteins. Thanks to the concerted kinase activity of cyclin E-cyclin dependent kinase 2 (CDK2) and Dbf4-dependent kinase (DDK)<sup>14,15</sup>, MCM10 is recruited to the pre-RC and CDC6 is replaced by the GINS complex and CDC45, that together with the MCM2-7 constitute the CMG complex <sup>16-18</sup>. This is called the pre-initiation complex (pre-IC). Activation of the CMG complex by cyclin A-CDK2 result in the unfolding of the DNA helix and facilitates the loading of processivity factor – proliferating cell nuclear antigen (PCNA), DNA polymerases and accessory factors which complete the replisome assembly and fires the process of DNA synthesis in the transition between G1/S <sup>16,18,19</sup>. CIZ1 helps coordinate the sequential functions of cyclin E- and A-dependent protein kinases and interacts directly with cyclins E and A <sup>20,21</sup>, with CDK2, and with p21<sup>Cip1</sup> <sup>5</sup>(Fig. 1.1). It also plays an indirect role in DNA replication by modulating the expression of genes, including cyclin D, that influence cell proliferation <sup>22,23</sup>.

### 3. mRNA and protein domain architecture of CIZ1.

Human full-length CIZ1 transcript is composed of 17 exons (Fig. 1.2A) where the different exons discovered in an exon-junction microarray analysis have never been found in translated CIZ1 <sup>24</sup>. At protein level, human CIZ1 protein is composed of 898 amino acids (aa) and is divided in two main functional domains (Fig.1.2B). It has been described that CIZ1 capacity of anchoring to the NM resides in its C-terminal third (Anchoring Domain, AD), which includes three C2H2-type zinc fingers and a matrix 3 homology domain <sup>8</sup>. CIZ1 DNA replication activity resides in its N-terminal fraction (Replication domain, RD) which includes two poly-Q regions and several cyclin-binding motifs <sup>20</sup> (Fig. 1.2B). Therefore, the first role described for CIZ1 was to regulate the temporally and spatially coordinated cyclin function during the assembly and activation of the DNA replication machinery <sup>20,21</sup>.

A

Human CIZ1 transcript:



B

Human CIZ1 protein:

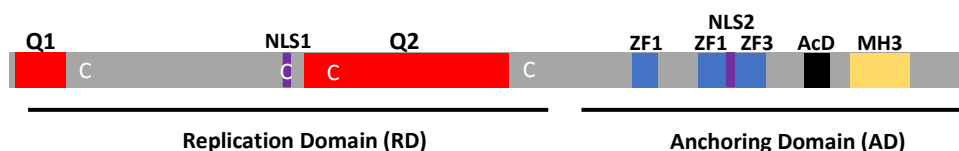


**Figure 1.2: Human CIZ1 structure.** A) CIZ1 scaled exonic structure. Grey: untranslated exon 1 variants. Coloured: translated exons. B) CIZ1 protein structure. Q: Glutamine-rich domain, NLS: Nuclear localisation sequence. ZF: Zinc finger. AcD: Acidic domain. MH3: Matrin 3 homology domain. CIZ1 functional domains are indicated. 'C': K/RXL cyclin-binding motifs.

#### 4. CIZ1 facilitates Xist localization to the inactive X-chromosome.

A second role discovered for CIZ1 is directly related with X-chromosome inactivation (XCI). In mammals, XCI randomly affects the paternal or maternal X-chromosome in females, acting as an evolutionary mechanism to compensate the genetic dosage for X-linked gene products between sexes<sup>25</sup>. This inactive state is then stably inherited through subsequent cell divisions. The initiation of XCI is controlled by a region of the X-chromosome called X-inactivation center (Xic), from which the long-noncoding RNA *Xist* is transcribed and accumulated in *cis*<sup>25</sup>. It has been described that *Xist* colocalizes with prechromatin areas that correspond to the NM<sup>26</sup>. *Xist* RNA spreading around the future inactive X chromosome (Xi) modifies the chromosome architecture, including sequential chromatin modifications that starts with the loss of histone modifications associated with active chromatin such as H3K9 acetylation and H3K4 methylation<sup>27</sup>. Subsequently, the X chromosome is hypoacetylated for H4 and enriched in repressive chromatin modification such as H3K27me3 and H3K9 me2<sup>28</sup>. The Polycomb group protein Ezh2 appears to be the histone methyl transferase responsible for trimethylation of H3K27 and has been reported to have some H3K9 methylation activity<sup>29</sup>.

Recent studies have revealed that CIZ1 is recruited to the Xi by *Xist* during the earliest stages of XCI, accumulating at high-intensity domains in the nucleus of female human or mouse cultured fibroblasts<sup>30</sup>. Immunolocalization of CIZ1 also overlaps with H3K27me3 marks and not with the active chromatin mark H3K4me3. Consistent with a role for CIZ1 at the Xi, RNA-FISH analyses of *Xist* in CIZ1-null mouse fibroblasts revealed a dispersed *Xist* signal throughout the nucleus instead of an accumulation at Xi<sup>30</sup>. Interestingly, the lack of overt developmental defects in *ciz1*<sup>-/-</sup> male and female mice suggests that CIZ1 is not required for the establishment of the repressive state of Xi because this is known to be essential. However, progressive infirmity was observed in female CIZ1-null mice from 9 months onward, showing abnormally enlarged primary and secondary lymphoid tissues (spleen, lymph node, lung and liver), evidencing a post-developmental function of CIZ1 at Xi<sup>30</sup>.

Further research revealed that CIZ1 interacts in an RNA-dependent manner with NM at Xi for most of the cell cycle, and that in S phase it shifts to an interaction that is not dependent on RNA<sup>31</sup>. This study also proved that the lack of CIZ1 alters the repressive gene regulation activity of

the polycomb repressive complex (PCR1/2), and linked CIZ1 with changes in nuclear position of XI during S phase <sup>31</sup>. Altogether, these results led to a model in which CIZ1 is part of a process that supports the meeting of enzyme and template during maintenance of Xi heterochromatin in cycling differentiated cells.

## 5. CIZ1 aberrant expression and cancer.

CIZ1 is expressed in a wide range of tissues <sup>32</sup>, and it is known to yield at least 22 alternatively spliced transcripts <sup>24</sup>. Although most of these transcripts are not well characterised, CIZ1 aberrant expression has been extensively linked with different human pathologies ranging from different types of muscular dystonia <sup>33,34</sup> to Alzheimer's disease <sup>35</sup>. Nevertheless, the main human pathology with which CIZ1 is associated is cancer. CIZ1 is linked with tumour growth in small cell (SCLC) and non-small cell lung carcinoma (NSCLC)<sup>36,37</sup>, breast<sup>23,38</sup>, colorectal<sup>39,40</sup>, prostate<sup>41</sup>, hepatocellular carcinoma<sup>42,43</sup>, gall bladder cancer<sup>44,45</sup> and tongue hemangioma<sup>46</sup>. In each case, cancer-specific alterations result in increased CIZ1 protein levels, or alternative splicing of Ciz1 transcript (Table 1). An exhaustive summary of studies implicating CIZ1 in human disease is shown in Appendix 1.

**Table 1. CIZ1 is associated with tumour growth in multiple cancers (updated version of <sup>13</sup>).**

Cancer	Cancer-Specific Ciz1 alteration	Mode of intervention	Result of intervention	Ref.
Lung cancer	Alternative splicing	shRNA	Reduced tumour growth in xenograft model	36,37
Colorectal carcinoma	Overexpression	siRNA	Reduced proliferation, and colony formation in vitro	39
Gall bladder carcinoma	Overexpression	siRNA	Reduced xenograft tumour growth. Reduced tumour migration in vivo	44,45
		shRNA	Suppressed proliferation by inducing apoptosis in vitro	
Prostate cancer	Overexpression	siRNA	Reduced tumorigenesis in xenograft models, reduced proliferation, G1 checkpoint activation	41
Breast cancer	Overexpression	siRNA	Reduced tumorigenesis, proliferation and anchorage dependence	23,38
Breast cancer	Overexpression increases estrogen sensitivity	Ciz1 overexpression	Increased estrogen sensitivity and increased tumour size in xenograft models.	38
Hepatocellular carcinoma	Overexpression	Ciz1 overexpression	Increased proliferation, migration	42,43
		siRNA	Reduced growth, tumorigenesis, metastasis	
Tongue Hemangioma	Overexpression	shRNA	Reduced proliferation and migration in vitro	46

shRNA: short hairpin RNA; siRNA: short interfering RNA

These studies have also reported that the deregulation of CIZ1 at transcript and protein level is involved in proliferation, invasiveness and anchorage-independent growth of cancer cell lines in vitro<sup>36-46</sup>. Despite the level of descriptive evidence that has emerged, the molecular basis by which CIZ1 aberrant activity may function as a tumour driver remains elusive.

## 6. CIZ1, Xi epigenetic instability and breast cancer.

The disappearance of the Xi is considered a hallmark of cancer, although it is currently under discussion whether this is due to epigenetic instability or genetic loss<sup>47</sup>. So far, only genetic instability had been clearly pointed to a cause of Xi loss, with past work implicating BRCA1<sup>48</sup>. Studies in different types of breast cancer revealed that the Xi epigenetic landscape also exhibits aberrant chromatin hallmarks, including a marked lack of H3K27me3 enrichment and the presence of H3K9 and H4 acetylation<sup>47</sup>. A set of X-linked genes that specifically escape from repression in breast cancer cell lines were also described. Altogether, this body of data suggests a highly perturbed transcriptional and chromatin status of the Xi in the context of breast cancer.

It has been previously suggested that the X chromosome inactivation has a role in the development of cancer<sup>49</sup>. In the particular case of breast cancer, previous studies have reported misbehaviour of *Xist* in breast cancer cells<sup>50</sup>, although these studies focused on the relation between BRCA1 and *Xist*. As we have discussed above, CIZ1 aberrant expression is linked with altered PRC1/2 activity resulting in abnormal epigenetic status and gene expression<sup>31</sup>. Additionally, CIZ1 overexpression is linked with all common solid tumours tested<sup>33-42</sup>, and there is a growing number of CIZ1 cancer-specific alternative transcripts<sup>51,52</sup>. This body of evidences points to CIZ1 as a candidate for Xi epigenetic disruption as a tumorigenic event. Nevertheless, to the best of my knowledge, the relation between a deficient CIZ1 activity in the maintenance of the Xi epigenetic landscape and the development of breast cancer remains completely uninvestigated.

## 7. Hypothesis and aims.

The working hypotheses of this study are:

- CIZ1 expression is aberrant in breast cancer cells and contributes to the development of some of the key features of the disease.
- Cancer-specific CIZ1 species have the capacity to disrupt normal CIZ1 activity in the maintenance of the Xi epigenetic landscape in a dominant negative fashion.

The research goals of this study are:

- i. To examine CIZ1 behaviour in a panel of breast tissue-derived cells.
- ii. To profile the expression of CIZ1 variants at transcript and protein level throughout the cell series.
- iii. To investigate whether expression of one or more cancer-associated CIZ1 variants in normal breast epithelial cells can recreate some of the aberrant features of Xi seen in aggressive breast cancers.

## Chapter 2. Materials and methods

---

### 1. Cell culture.

#### 1.1. Human cell lines used.

The cell lines MCF7 and MCF10A were tested and authenticated in August 2017 using PCR-single-locus-technology (Eurofins Medigenomix Forensik GmbH), the last being a kind gift from I. Wood, University of Leeds. BT-474, SKBR-3 and MDA-MB-231 cells were a kind gift from Dr W. Brackenbury, University of York. 1-7 HB2 cells were a kind gift from Prof V. Speirs, University of Aberdeen. For all cell lines, a cell pellet sample was stored for future authentication if necessary.

**Table 2.1 Cell line information.**

Cell line	Derivation	BRCA1 status	Sex	Cancer derived?
<b>MCF-7</b>	Metastatic breast adenocarcinoma	Wild-type	Female	Yes
<b>BT-474</b>	Metastatic breast adenocarcinoma	Wild-type	Female	Yes
<b>SKBR-3</b>	Metastatic breast adenocarcinoma	Wild-type	Female	Yes
<b>MDA-MD-231</b>	Metastatic breast adenocarcinoma	Wild-type	Female	Yes
<b>MCF10A</b>	Mammary Gland epithelium	Wild-type	Female	No
<b>1-7 HB-2</b>	Mammary Luminal epithelium	Wild-type	Female	No

#### 1.2. Primary cells.

Three independent populations of female Primary Human Mammary Epithelium cells (HPMECs, passage 1) were used in this study. These cells were kindly donated by Breast Cancer Now.

### 2. Maintenance.

Cells were grown at 37°C in a humidified atmosphere in 5% CO<sub>2</sub> air on plastic culture plates (Scientific Lab. Supp.). Primary cells were grown on collagen-I coated plastic plates (BioCoat, Cat. No. 734-0109) . Cells were usually kept at approximately 80% confluent density and passaged when necessary. Passaging was done by removing media, washing with warm Dulbecco's

phosphate buffered saline (D-PBS, Gibco) and cells lifted them with 1mL of 1x 0.5 % Trypsin-EDTA (10X) (Gibco). Trypsin was quenched with serum in fresh medium and cells split onto new plates as appropriate. Primary cells were only passaged one time when necessary. Cells stocks were frozen in appropriate medium with 10% dimethyl sulphoxide (DMSO) and stored in liquid N<sub>2</sub>.

## 2.1. Media.

Penicillin, streptomycin and glutamine (PSG) were added to all media (10 U/ml, 10µg/ml, 2,92 mg/ml final concentration respectively). Unless otherwise stated all media were obtained from Gibco® (Invitrogen) and other chemicals obtained from Sigma-Aldrich. Mammary Epithelial Cell Growth Medium (MEGM) Kit was obtained from Lonza (Catalog No. CC-3150). Fetal bovine serum (FBS) was obtained from Biosera for all cell lines media but primary cells, for which FBS from PAA Laboratories was used.

**Table 2.2 Details of cell culture media for cell lines used.**

Cell line	Media	Supplements
<b>MCF-7</b>	EMEM	10% FBS
<b>BT-474</b>	DMEM	10% FBS
<b>SKBR-3</b>	DMEM	10% FBS
<b>MDA-MD-231</b>	DMEM	5% FBS
<b>MCF10A</b>	MEGM	5% Horse serum, human epidermal growth factor (hEGF) 20 ng/µl, human recombinant insulin 10 µg/ml, hydrocortisone 500 ng/ml.
<b>1-7 HB-2</b>	DMEM	10% FBS
<b>HPMECs</b>	DMEM:F-12K	10% FBS, hEGF 10 ng/ µl, human recombinant insulin 5 µg/ml, hydrocortisone 500 ng/ml, apo-transferrin 10µg/ml.

DMEM - Dulbecco's Modified Eagle's Medium

EMEM - Eagle's Minimum Essential Medium

F-12K - Kaighn's Modification of Ham's F-12 Medium

## 3. Immunofluorescence.

Cells were grown on glass coverslips to 80-90% confluence and bathed in CSK buffer (PIPES buffer pH6.8 10mM, NaCl 100mM, Sucrose 300mM, MgCl<sub>2</sub> 1mM, EGTA 1mM) with 0.1% Triton-X-100 (CSKD) for 1 min prior to fixation in 8% paraformaldehyde (PFA). After fixation cells were rinsed twice with PBS then incubated for 15 min in BSA Antibody buffer (0.02% SDS, 0.1% TX100, 10 mg/ml nuclease-free BSA (Jackson, Cat. No. 001-000-162) in PBS), followed by 2 hr at 37 °C

with primary antibody (in BSA antibody buffer). After three washes in the same buffer, anti-species secondary antibodies were applied (Alexa Fluor 488 or 568) for 1 hr, followed by three further washes. In all cases, cells were incubated in Hoechst 33258 (10 ng/mL; Sigma) for 5 min for DNA staining and then mounted in VectaShield® (Vector Laboratories). All antibodies and dilutions are listed in table 2.6.

### 3.1. Nuclear matrix extraction.

Where indicated, coverslips were subjected to nuclear matrix extraction prior to immunofluorescence in order to identify the extractability profile of the different CIZ1 fragments following standard protocol<sup>53</sup>. Culture media was removed and cells were washed with CSK-D (CSK with 0.1% Triton-X-100) for 1 min. Subsequent coverslips were washed with CSK-DS (CSK-D buffer with 0.4M NaCl) for 1 min. Cells were then rinsed with nuclease buffer (TBS 0.05% Triton-X-100 5% BSA), and then incubated with DNase and RNase-containing nuclease buffer independently for 1 hr at 37°C. Cells were then rinsed again with CSK-DS to remove free nucleotides and ribonucleotides. A fraction of the cells were fixed after CSK-D, CSK-DS and nuclease buffer rinse steps using 8% PFA for 15 min, and then washed 3 times in PBS for 5 min each prior to immunofluorescence.

### 3.2. Plasmid DNA transfection.

1-7 HB2 cells were grown on coverslips to 75% confluence prior to the transfection in 24-well culture plates (Scientific Lab. Supp.). Cells were then transfected with approximately 500 ng of the chosen GFP-tagged *Ciz1* DNA construct (Table 2.3) together with 50 µl of Opti-MEM I Reduced-Serum Medium (ThermoFisher, Cat. No. 31985062) and 1.5 µl of the transfection reagent TransIT-X2 reagent (Cambridge Bioscience, Cat. No. MIR6003). Cells were imaged 22 hr after transfection as described above. For image processing, ImageJ Fiji 1.52p software was utilized.

**Table 2.3 CIZ1 transfection constructs.**

Construct	Origin	Structure	Provided by
GFP-N57	Mouse	N-terminus polyQ region	Holliman, S.
F-Variant GFP-CIZ1	Human	Full-length CIZ1 (Δ exons 9-11, Δ part of exons 8 and 12)	Swarts, D.

### 3.3. Imaging.

Fluorescence images were captured using a Zeiss Axiovert 200M fitted with a 63×/1.40 Plan-Apochromat objective and Zeiss filter sets 2, 10, 15 (G365 FT395 LP420, BP450-490 FT510 BP515-565, BP546/12 FT580 LP590), using AxioCam 506 mono and AxioVision image acquisition software (SE64 release 4.9.1). Where changes in fluorescence intensity are quantified across an extraction series, coverslips were imaged as a set with all images for each filter set captured with the same exposure time. For presentation, images were enhanced using ImageJ Fiji 1.52p or Affinity Photo 1.4.1, maintaining identical manipulations across extraction series so that image intensities reflect actual relationships. All quantification of image intensity was carried out prior to manipulation. For the presentation of images illustrating positional, rather than intensity information, images were not necessarily modified identically.

### 3.4. Statistical analysis.

The statistical significance of the pixel intensity differences measured in transfected and untransfected cells in Chapter 5 was calculated using a Student's T-distribution with 2 tails and degree of freedom equal to 2, utilising the software Microsoft Excel, from Microsoft Office 365 package (release 16.0).

## 4. RNA analysis.

### 4.1. Total RNA extraction.

RNA homogenization was achieved using 2mL of TRIzol Reagent (Ambion Life Technologies, Cat. No. 15596-026) per 9 cm plate of cells at 80-90% confluence. The phase separation step involved addition of chloroform and isolation of aqueous phase followed by RNA precipitation with 100% isopropanol and a final RNA wash step with 75% ethanol. RNA was then resuspended in DEPC water. RNA quality and concentration were tested by spectrophotometry using NanoDrop™ (ND-1000). RNA integrity was tested by direct observation in 0.8% w/v agarose electrophoresis gel.

## 4.2. Reverse Transcription Quantitative PCR (RT-qPCR).

Expressions levels of CIZ1 domains were analysed using real-time retrotranscribed quantitative PCR. cDNA was generated using SuperScript<sup>®</sup> III Reverse Transcriptase (ThermoFisher Scientific, Cat. No. 18080044). RT-qPCR was carried out using Applied Biosystems<sup>™</sup> Fast SYBR<sup>™</sup> Green Master Mix (Cat. No. 10381275) and domain-specific CIZ1 primers (Table 2.5), using a CFX96 Real-Time PCR Detection System (BioRad). 300ng/ $\mu$ l of sample cDNA was used per reaction. Primers were used at 200nM. The following program was used: 95 °C for 30sec, followed by 40 cycles of 95 °C for 3 sec and 60 °C for 30 sec. Data was analysed using the Bio-Rad CFX Manager 3.1 software (Biorad).

The relative quantification of gene expression was done using the  $2^{-dCt}$  where expressed as percentage of GAPDH expression level (data not shown), or  $2^{-ddCt}$  formula<sup>54</sup> where indicated. When using the or  $2^{-ddCt}$  formula, fold changes of gene expression were normalized to an average of the primary cells expression levels.

## 4.3. Northern blotting.

Northern blot analysis was performed using NorthernMax-Gly kit (Invitrogen, Cat. No. AM19460) as per manufacturer's instructions. Digoxigenin labelled RNA probes were generated from T7 DNA templates with MEGAscript<sup>™</sup> Transcription Kit (Ambion, Cat. No. AM1354) using Dig-UTP and NTP mix with reduced UTP concentration. RNA was purified with MEGAclear<sup>™</sup> Kit (Ambion, Cat No. AM1908). RNA size and integrity were analysed by running the RNA sample on denaturing 8M Urea, 5% PAGE (not shown). The primers used for DNA template generation are summarized in Table 2.4. The sequence of the probes can be found in Table 2.5.

For each sample, 5  $\mu$ g of total RNA was denatured and loaded using loading buffer containing glyoxal/dimethylsulfoxide (DMSO) as denaturing agent, then separated on 1% (w/v) LE-agarose electrophoresis gel. The RNAs were then transferred to Hybond-N+ nylon membranes (GE Healthcare) by capillary blotting and fixed by UV-crosslinking. (2x120 mJ). Blots were pre-hybridised in UltraHyb<sup>®</sup> for 30 min at 65 °C, and hybridised with 0.4 nM of probe O/N at 65°C. The membranes were washed once in 2xSSC/0.1% (w/v) SDS for 10 min at RT and twice in 0.1xSSC/0.1% (w/v) SDS for 20 min at 68 °C for AD probe and 72 °C for RD probe. DIG detection was performed with an alkaline phosphatase coupled anti-DIG antibody (Roche, Cat No.

11093274910), a DIG Wash and Block Buffer Set (Merck, Cat. No. 11585761001), and the chemiluminescence substrate CSPD (Roche) according to the manufacturer's instruction (Roche, Cat. No.11585762001). The signals were visualized using Syngene PXi chemiluminescence imaging system. The software ImageJ Fiji 1.52p was used for both, signal intensity analysis and edition of the images for illustration purposes. All quantification of image intensity was carried out prior to manipulation.

#### 4.4. Primers and probes.

**Table 2.4. Primers for qPCR and probe design.**

Primer	Sequence (5'-3')	Exon/Gene
RD Forward	ACACACCAGAAGACCAAGATTTACC	hCiz1 Exon 6/7 junction
RD Reverse	TGCTGGAGTGCCTTTTCT	hCiz1 Exon 7
AD Forward	CGAGGGTGATGAAGAAGAGGA	hCiz1 Exon 14
AD Reverse	CCCCTGAGTTGCTGTGATA	hCiz1 Exon 16
GAPDH Forward	CTCTCTGCTCCTCTGTTCCGAC	Human <i>Gapdh</i>
GAPDH Reverse	TGAGCGATGTGGCTCGCT	Human <i>Gapdh</i>
RD probe template forward	TGCAACAGTCTTTCCCAAGC	Exon 5
RD probe template reverse	TAATACGACTCACTATAGGGAGTGCCTTT TTCCTTGCGC	Exon 7 + T7 promoter
AD probe template forward	CAGTGGACGCTGTGGGTTGC	Exon 14
AD probe template reverse	TAATACGACTCACTATAGGGACTTGCA GTGGGAGAGC	Exon 16 + T7 promoter

**Table 2.5. Probes for Northern blot analysis.**

Primer	Sequence (5'-3')
RD probe	GGAGTGCCTTTTCTTGGCGATGTCCTCTGGGCAGGGCGGTAAATCTTGGTCTTCTG GTGTGTCCATCCGGGGCTCTGCGCTTCTCAGACCCCTCTGGGGGTCTGACTTGTG TTCCACAGGCATTGTCTGAGAAGAAGAATCCTTTCGATTGGGGGTGGTAGAGGAGGA GGTCCGGGCTGTTTCTGGGGTCCGTCCTGAAAGTTGAACTGGGAAGGGTTCAT GGGGACCCCAACAGGAGGAGTCCAGCAAGGACTGGCGAGTGGCCTGGGAAAGAA CTGTTGCA
AD probe	GGGACTTGCACTGGGAGAGCTGTGCCCTGAGTTGCTGTGATAGAAGTGTGGCAGA TGCGGCAGATATAGCCATCACGGGCACCAGGAAGTCCACACCATATGCAGTATTGG GGCTGTAGGTCTCCGAGCCCTTCCACTCCTCTGGATATATCTCTGGACCTCACCTG CTTGACAGATTCTCCTCAACCTCGATCTTCTTTCATCCTCATCATCCTCTTCTCTT CTTCATCACCCCTCGAAGCAACCCACAGCGTCCACTG

## 5. Protein analysis.

### 5.1. Total protein lysates form cells.

For total protein lysates, cells grown on culture plates were washed twice with cold D-PBS, drained for 1 min and then 250µl of loading buffer was added from a 4x stock of 16% W/v SDS, 10% W/v glycerol, 250mM β-mercaptoethanol, 0.004% w/v bromophenol blue, 65.5 mM tris-HCL pH 6.8. Cells and buffer were then scraped into cold microcentrifuge tubes and brought to a concentration of 2x with 250 µl of ultrapure water. Samples were vortexed and heated at 90 °C for 10 minutes, then aliquoted as needed and stored at –80 °C.

### 5.2. SDS-PAGE gels and transfer.

Total protein lysates were separated using 4-15% acrylamide gradient SDS-PAGE precast gel (Mini-PROTEAN® TGX, Biorad, Cat. No. 456-1085). 20 µl of sample was loaded for primary cells, 10 µl for normal cell lines, 5 µl for cancer cell lines and marker. Equivalent protein load in every lane was verified using Histone 3 detection as load control. Gels were run in Tris Glycine SDS running buffer (0.025 M Tris, 0.192 M glycine, 0.1 % w/v SDS). PageRuler™ Plus Prestained Protein Ladder (Biorad, Cat. No. 26619) was used as a size marker.

Separated proteins were transferred onto Invitrogen™ Novex™ iBlot™ Nitrocellulose Transfer Stack (Invitrogen, Cat. No. 12289309) using iBlot™ (Invitrogen) semi-dry blotter programme P2, 6 minutes. Membranes were stored at -20 °C.

### 5.3. Western blotting.

For western blotting analysis, membranes were blocked with milk or BSA blocking buffer depending on antibodies (Table 2.6) for 30-45 minutes, then incubated with primary antibody in blocking buffer for 2 hr at RT or O/N at 4 °C. Membranes were washed three times, each for 10 min in blocking buffer then incubated with the appropriate secondary antibody (horse radish peroxidase (HRP) anti-mouse or anti-rabbit) in blocking buffer for 1hr at RT. Membranes were then washed three times in wash buffer (as blocking buffer without milk or BSA). Blots were imaged using 1:1 mix of EZ-ECL A and B detection reagent (Thermo Fisher, Cat. No. 32109) with a Syngene PXi chemiluminescence imaging system.

## 5.4. Immunoprecipitation

For antibody specificity testing, immunoprecipitation of CIZ1 was performed following a standard pre-immobilised antibody approach protocol. Mouse anti-CIZ1-AD monoclonal '1794' antibody was pre-immobilized onto Pierce™ Protein A/G Agarose beads (ThermoFisher, Cat. No. 20421) and then incubated with HB2 1-7 total cell lysates. Beads were collected by centrifugation and removed from the lysates. Wash steps were performed after each incubation step. Elution and denaturation of the proteins were performed by heating the beads in sample loading buffer followed by SDS-PAGE protein separation and western blotting analysis of the captured protein utilising the monoclonal mouse anti-CIZ1-RD antibody 'Bella'.

## 5.5. Antibodies.

Unless otherwise stated, all mouse antibodies were monoclonal, and all rabbit and goat antibodies were polyclonal.

**Table 2.6. Details of antibodies used, buffers and incubation times.**

	Western blot			IF
Antibody	Dilution	Blocking buffer	Time/T°	Dilution
Mouse Bella (anti-human CIZ1)	1:10	TBST BSA	O/N 4 °C	1:25
Rabbit Nov4 (NB100-74624, Novus)	1:1000	PBST milk	O/N 4 °C	1:1000
Rabbit $\alpha$ -histone H3 (ab1791, Abcam)	1:10,000	PBST milk	2 hr RT	-
Mouse 87 (anti-human CIZ1)	-	-	-	1:20
Rabbit 1794 (anti-mouse CIZ1)	-	-	-	1:1000
Goat $\alpha$ -rabbit HRP (ab6721, Abcam)	1:10,000	As primary	1 hr RT	-
Goat $\alpha$ -mouse HRP (ab6789, Abcam)	1:10,000	As primary	1 hr RT	-
Goat $\alpha$ -mouse Alexa Fluor <sup>®</sup> 488 green	--	-	-	1:1000
Goat $\alpha$ -rabbit Alexa Fluor <sup>®</sup> 568 red	-	-	-	1:1000
Mouse H3K27Me3 (ab6002, Abcam)	-	-	-	1:2000

<b>Rabbit <math>\alpha</math>-H2AK119Ub1 (D27C4, CST)</b>	-	-	-	1:1000
<b>Mouse <math>\alpha</math>-Fibrillarlin (ab4566, Abcam)</b>	-	-	-	1:100
<b>Mouse <math>\alpha</math>-Lamin B2 (33-2100, Invitrogen)</b>	-	-	-	1:100

PBST milk – 10% w/v non-fat dried milk (Marvel), 1 x phosphate buffered saline (PBS, Sigma), 0.1% tween-20

TBST BSA – 5% w/v BSA, 1 x tris buffered saline (TBS, Sigma) 0.05% tween-20

**Table 2.7 Anti-CIZ1 antibodies, sources, antigens and known behaviours.**

<b>Antibody</b>	<b>Immunogen</b>	<b>Selection</b>	<b>Source</b>	<b>Notes</b>	<b>Xi reactive</b>
<b>Bella (anti-human CIZ1)</b>	Synthetic peptide (RD)	Synthetic peptide (RD)	Coverley lab	Reactive with linear epitope (SS unpublished)	No in mouse
<b>Edward (anti-human CIZ1)</b>	Recombinant fragment (AD, native multimeric)	Recombinant fragment	Coverley lab	Reactive with multimeric purified protein. Poorly reactive with linear epitope (GT unpublished).	No in mouse
<b>Nov 4 (anti-human CIZ1)</b>	Recombinant protein	Synthetic peptide (AD)	Novus	Reactive with linear epitope, but epitope is subject to proteolytic cleavage in vivo (SS unpublished)	Yes in mouse and human
<b>87 (anti-human CIZ1)</b>	Recombinant fragment (AD, native multimeric)	Recombinant fragment	FDAB	Mapped and peptide reactive <sup>53</sup> and LW unpublished.	Yes in mouse and human
<b>1794 (anti-mouse CIZ1)</b>	Recombinant protein (RD)	Recombinant protein (RD)	Coverley lab	Multiple bands with preference for large forms <sup>7</sup> .	Yes in mouse and human

## Chapter 3. Immunofluorescence analysis of CIZ1 expression in breast cancer

---

### 1. Introduction.

Previous work in female murine cells has shown that CIZ1 localises in one or two high-intensity domains within the nucleus, when detected by immunofluorescence via epitopes in both N-terminal RD<sup>7,55</sup> or C-terminal AD<sup>56</sup>. It is also seen in smaller foci throughout the nucleus of both male and female cells. When detected in either culture-adapted (MEF) or primary (PEF) embryonic fibroblasts from female mice, CIZ1 domains appear as a discrete entity, in contrast with cancer-derived cell lines where its locations are more irregular and dispersed<sup>57</sup>. Further studies revealed colocalisation of CIZ1 with discrete accumulations of repressive chromatin marks such as H3K27me3 and H2AK119Ub in PEFs and some human female cell lines, suggesting that CIZ1 accumulates at the inactive chromosome X (Xi) in female cells also<sup>57</sup>. Additionally, there are a growing number of studies that link altered CIZ1 expression with different human pathologies including most of the common solid tumours<sup>13,36,38,40-42,58-60</sup>. While there are strong evidences of aberrant nuclear organization, morphology and expression levels of genes on the Xi in cancer<sup>49</sup>, specially in breast cancer cells<sup>47</sup>, the contribution of a corrupted Xi epigenetic landscape to the tumorigenic event is poorly understood. The purpose of this study is, using CIZ1 role in maintenance of the Xi epigenetic status as a model, to investigate the relation between CIZ1 activity and breast cancer progression.

## 2. Aims.

The aims in this chapter are to:

- i. Select a panel of cell lines representative of the different stages and molecular subtypes of the breast cancer progression, ranging from the primary state to the metastatic and more aggressive stage.
- ii. Validate the results of previous studies with mice cells in human cells.
- iii. Investigate the relation between CIZ1 accumulation at Xi and breast cancer progression.

## 3. Experimental design.

A bibliographic search was performed in order to select a panel of breast cancer cell lines representing the main stages of the disease progression, as well as culture-adapted non-cancerous cell lines suitable for this study. The breast cancer research charity Breast Cancer Now (BCN) was contacted and granted us access to primary mammary epithelial cells through a successful application to their steering committee, as well as internal ethics applications and a material transfer agreement between BCN and the University of York.

Immunolocalisation of CIZ1 via N-terminal and C-terminal epitopes (Fig. X MAPA CIZ1 in INTROO) was performed in order to analyse CIZ1 enrichment at the Xi. Colocalisation of CIZ1 with Xi markers and different nuclear components was performed.

## 4. Results.

### 4.1. Selected cells and cell lines represent the molecular subtypes of breast cancer, the culture-adapted non-cancerous state and the *basal state* of the human female breast tissue.

As with many other types of cancers, breast cancer is characterised by a high genetic and epigenetic heterogeneity<sup>61</sup>. Gene expression profiling has been widely utilised in order to catalogue breast cancer cell lines. The selection of breast cancer cell lines for this study was made based on the status of three receptors that have been conventionally used for breast



**Figure 3.1: Current subtyping schemes of breast cancer cell lines and cells used in this study.** A) Brightfield pictures of the cells used in this study. Size bar represents 100  $\mu\text{m}$ . B) Scheme of breast cancer cell lines subtyping based on molecular markers, ordered from less to more aggressive. C) Molecular status of the primary molecular markers ER, PR and HER2 of the breast cancer cell line subtyping [1] and nomenclature of the cell lines used in this study. NS: not studied; L: Luminal; B: Basal; LH+: Luminal-HER2+, BB: Triple negative/Basal-like B.

cancer subtyping : estrogen receptor (ER), progesterone receptor (PR), and human epithelial receptor 2 (HER2)(Figure 3.1A), which helps classify them into the nomenclatures luminal A, luminal B, HER2 positive, and triple negative subtypes (Figure 3.1B) <sup>62</sup>. For the purpose of this study, one cell line of each subtype was cultured according to recommended conditions (Figure 3.1C). From these, I generated total cell protein lysates, total RNA, DNA samples for future verification of cell identity prior to publication (banked), and culture media for mycoplasma testing.

In order to have a model for the “normal” state of the mammary epithelial cell, the non-cancerous cell line MCF 10A <sup>63</sup> was originally selected for this study. Based on the ambiguity that these cells exhibited between “cancer” and “normal” behaviour at both protein and RNA level, and upon the disagreement in whether they are a good model for “normal” state of the breast tissue (likely due to the expression of both epithelial and mesenchymal markers <sup>63</sup>), a second “normal” human female breast cell line (1-7HB2, Figure 3.1C) was included, following recommendation of Professor V. Spier’s, University of Aberdeen.

Considering that some of the activities of CIZ1 in maintenance of the epigenetic landscape have been revealed to be corrupted in differentiated fibroblasts in long-term culture <sup>31</sup>, three independent populations of passage 1 human primary mammary epithelial cells (HPMECs) were included in this study as a the “basal” state of the breast tissue (Figure 3.1 C). Total cell protein, total RNA and DNA samples were obtained in an equivalent way to the cancer lines.

It is important to note that, although the different molecular subtypes of breast cancer do not represent the different stages of the disease, these cell lines have been originally established from the different breast cancer types, thus encompassing a range of tumours that exhibit progressively poorer prognosis and increased aggressiveness. For this reason, the panel of breast cancer cell subtypes selected for this study represents the nearest approximation to a cell-line-based model in which we could evaluate the relative importance of CIZ1 biology at the different degrees of cellular proliferation and aggressiveness of the disease.

#### 4.2. CIZ1 accumulates at the Xi and might be implicated in Xi relocation during S-phase in HPMECs.

Previous studies in female mouse cells have revealed that CIZ1 accumulates at the Xi<sup>57,31</sup>. In order to validate this result in human breast cells, immunofluorescence analyses of CIZ1 N-terminal domain and the Xi markers H3K27me3 and ubiquitinylation of histone H2A<sup>29</sup> were performed in HPMECs and 1-7 HB2 cells (Figure 3.2A). Consistent with the previous literature, CIZ1 foci colocalised with an enrichment of both Xi marks, representing a strong evidence that CIZ1 accumulates at Xi in these cells.

Previous analyses of CIZ1-marked Xi in PEFs reported a shift in Xi location from the periphery of the nucleus to the nucleolar region during S phase that was lost in both CIZ1-null PEFs and culture-adapted mouse embryonic fibroblasts (MEFs)<sup>31</sup>. To further validate these results, immunofluorescence analyses scoring CIZ1-marked Xi location with respect to nuclear components with well-defined locations (fibrillarin at the nucleolus and lamin at the nuclear periphery<sup>64</sup>) were performed in HPMCs (Figure 3.2B, C). CIZ1 was found predominantly in the periphery of the nucleus although it also colocalised with the nucleolus in some cells, supporting the hypothesis that implicates CIZ1 in a mechanism underpinning Xi relocation in S phase suggested in the previous literature<sup>31</sup>. Together, these results support the idea that the role of CIZ1 in the Xi reported in PEFs is also occurring in primary human cells. Nevertheless, it is important to remark that all pictures analysed in this experiment belonged to two technical replications of the same sample of HPMECS. Thus, performing more independent biological repeats is highly recommended in order to support this result.

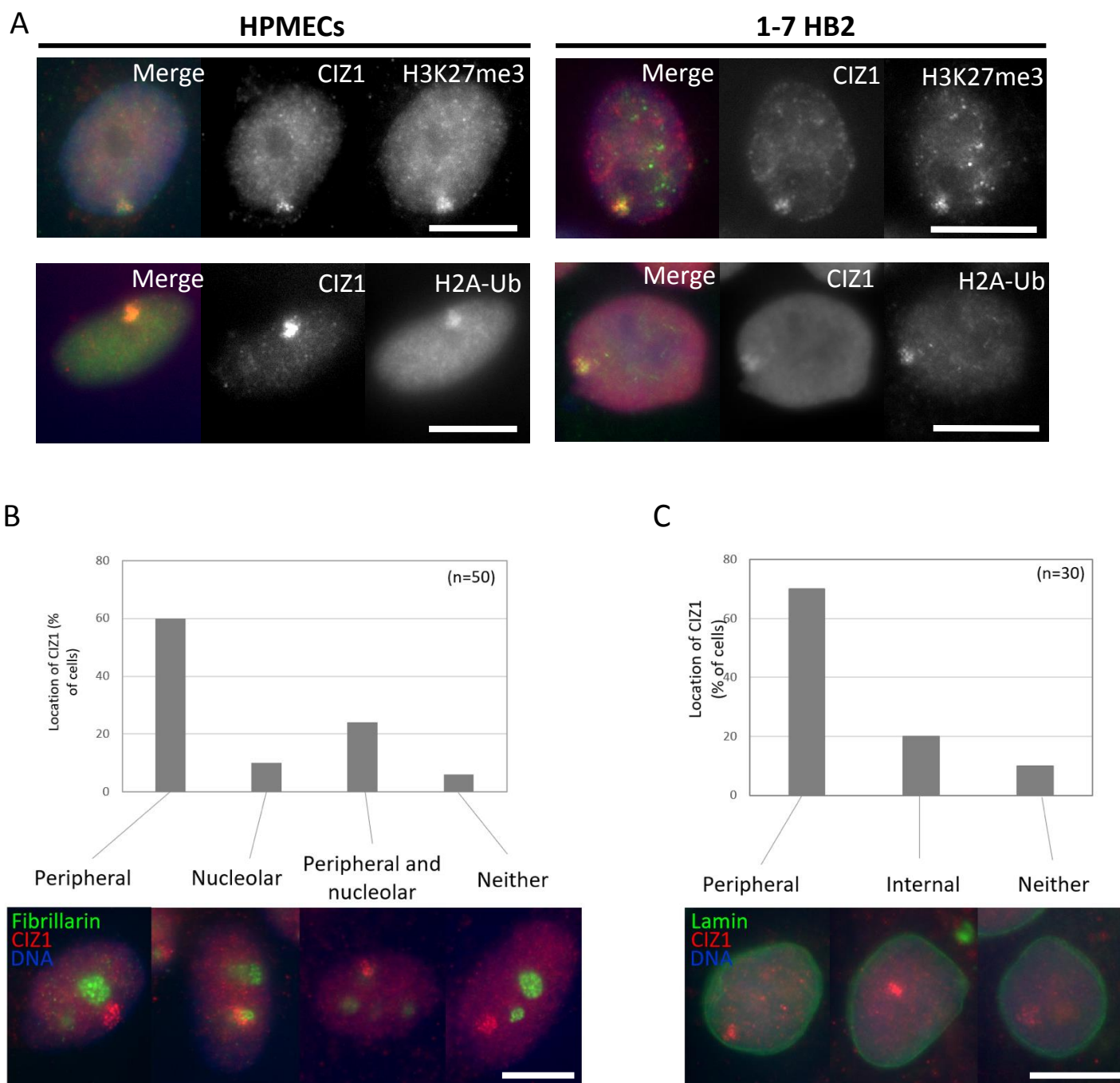


**Figure 3.2: CIZ1 colocalises with the Xi markers and presents a predominantly peripheral position in the nucleus of HPMECs and 1-7 HB2 cells.** A) Immunodetection of CIZ1 RD and the Xi marks H3K27me3 and H2A-Ub revealed a CIZ1 enrichment at the Xi the nucleus of HPMECs and 1-7 HB2 cells. All scale bars represent 10 microns. B) Immunofluorescence analysis of the relative position of CIZ1 (Red) respect to the nucleolar component fibrillarin (Green) (n= represents the number of cells counted from a single preparation but not the number of independent biological repeats counted, not allowing to include error bars). The predominantly peripheral localisation of CIZ1 with some cells presenting colocalisation with fibrillarin supports the idea that the Xi translocates to the nucleolar region during S-phase proposed in previous studies with mouse cells<sup>31</sup>. C) Immunofluorescence analyses of the relative position of CIZ1 (Red) respect to the nuclear matrix component lamin (Green) revealed similar results to the previous experiment and literature<sup>31</sup>.

#### 4.3. CIZ1 domains colocalise in foci in all HPMECs but only in some 1-7HB2 and MCF10A cells.

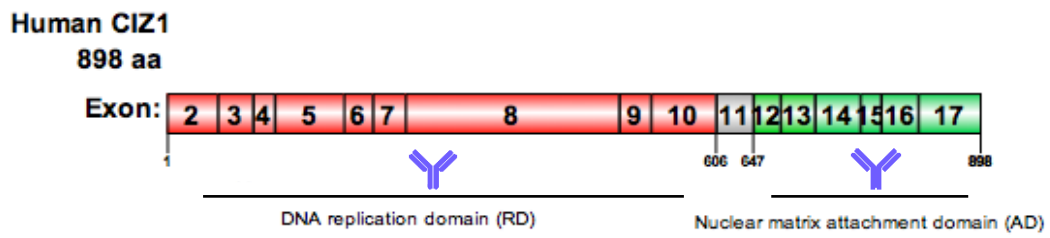
Consistent with the previous studies in mouse cells<sup>57,31</sup>, immunolocalisation of CIZ1 via epitopes in the N-terminal (RD) and C-terminal (AD) (Figure 3.3A) revealed a single discrete accumulation of both domains (CIZ1 patch), plus a signal throughout the nucleus in all HPMECs predominantly with anti-RD antibody (Figure 3.3B). Interestingly, the number of cells of the “normal” cell lines that exhibited CIZ1 foci was reduced compared to HPMECs. In the case of MCF10A cells, colocalisation of RD and AD was less evident and a significant reduction in CIZ1-RD predominance throughout the nucleus could be appreciated (Figure 3.3B). As discussed below, this pattern resembles one of cancer cells, raising concerns about the validity of MCF10A as a model for “normal” non-cancerous breast cell line.

In any case, the fact that CIZ1 localisation is substantially altered even in the non-cancerous cell lines indicates that CIZ1 physiological activity may be compromised during the process of culture-adaptation and immortalisation of the cells.

#### 4.4. CIZ1 foci disruption and lack of CIZ1 domain colocalisation in cancer cell lines.

CIZ1 immunolocalisation analyses performed under identical conditions in breast cancer cell lines revealed substantial differences in CIZ1 sub-nuclear localization and CIZ1 domain colocalisation between the different cancer stages (Figure 3.4A). While more or less discrete CIZ1 foci could be found in all cancer cell lines, CIZ1 signal was irregular and colocalisation of CIZ1 domains was heavily compromised in most of the cases. Only the low-grade breast cancer MCF7 cells exhibited evident colocalisation of CIZ1 domains plus a predominantly RD signal across the nucleus. This features highly resemble the immortalised “normal” 1-7HB2 cells, suggesting that CIZ1 is similarly compromised during the adaptation to sustained proliferation in either cancer or non-cancer-derived populations. For the rest of cell lines, CIZ1 foci consisted of almost exclusively of C-terminal AD. This separate detection of CIZ1 domains manifest what could be an event of “uncoupling” of CIZ1 domains. The implications of CIZ1 domains as independently expressed entities, or fragments of an unknown processing event, will be discussed later on this study.

A



B

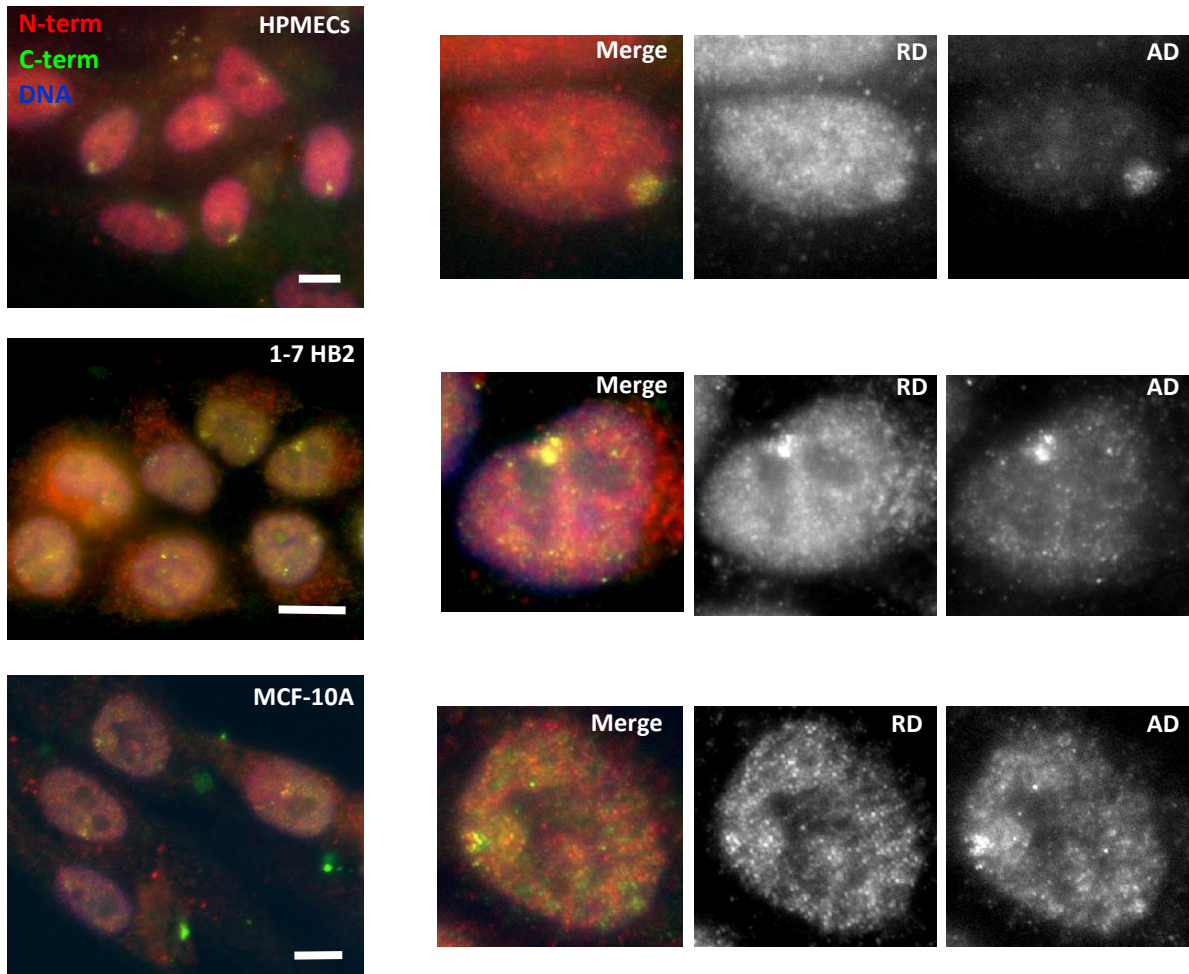
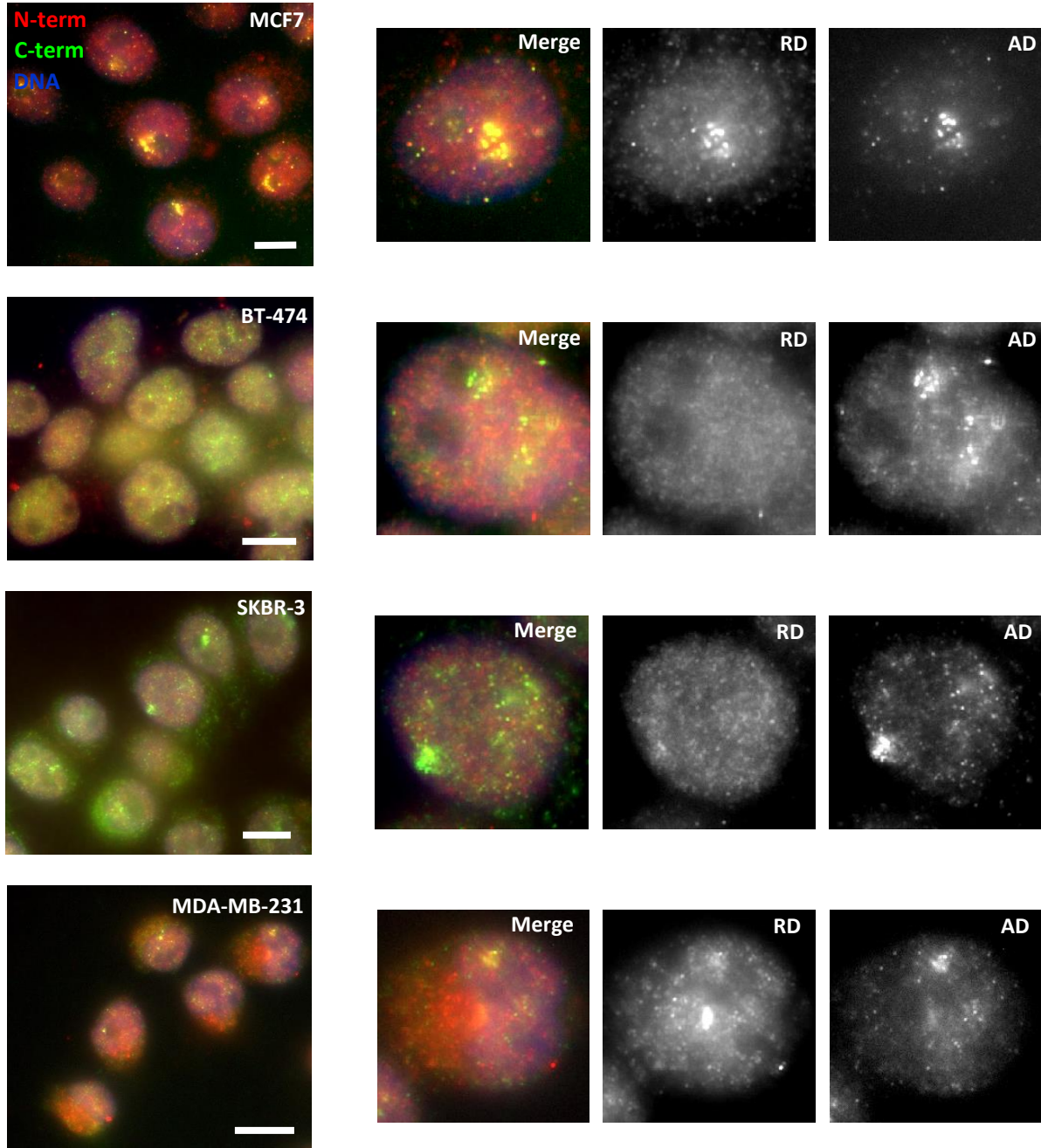


**Figure 3.3 CIZ1 domains colocalise in foci in all HPMECs but only in some 1-7 HB2 and MCF10A cells. A)** Representation of human full-length CIZ1. Numbers represent exons (exon 1 is not translated to protein<sup>7</sup>) and colours represent the limits of the domains used for the immunofluorescence analyses (Red: N-terminal RD; Green: C-terminal AD). **B)** Immunofluorescence CIZ1 RD and AD detection in detergent treated HPMECs, 1-7 HB2 and MCF10A cells. Left: Field showing multiple cells illustrates the reduced number and irregularity of CIZ1 foci present in cell lines. Right: Amplification of cell nuclei illustrate the differences in colocalisation of CIZ1 domains between cell types. Scale bars represent 10 microns.

A



B

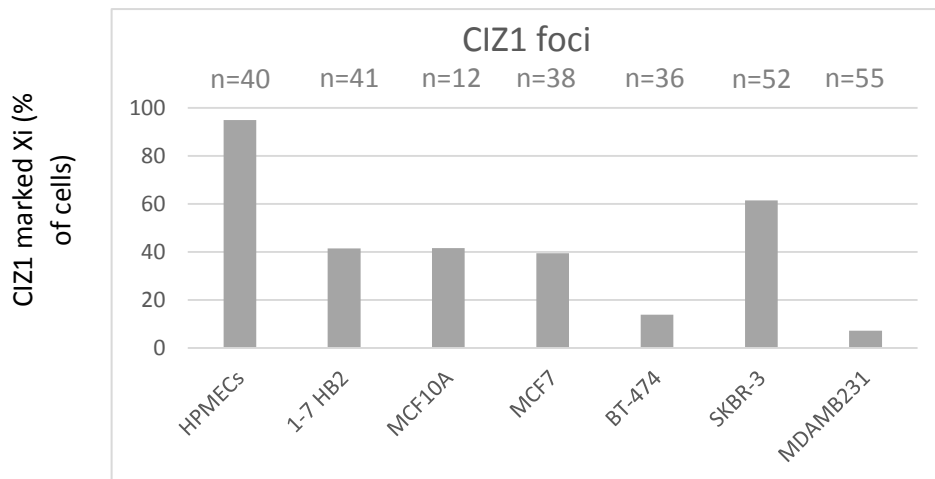


**Figure 3.4. CIZ1 location is highly altered in breast cancer cells cancer.** A) Immunofluorescence detection of CIZ1 RD (red) and AD (green) in detergent treated MCF7, BT-474, SKBR-3 and MDA-MB-231 cells reveals different locations for each domain. Left: Field showing multiple cells illustrates the variable number of cells exhibiting CIZ1 foci in cell lines. Right: Amplification of cell nuclei illustrate the differences in colocalisation of CIZ1 domains between cell types. Scale bars represent 10 microns. B) Estimation of CIZ1-marked Xi incidence throughout the cell series. Counts based on distinguishable discrete CIZ1 accumulation with CIZ1 domain colocalisation where possible. For BT-474 cells, counts were based upon CIZ1-AD accumulation exclusively. n= represents the number of cells counted from a single preparation. Absence of error bars is due to the lack of technical or biological repeats.

Although the irregularity and scattering of CIZ1 signal in most of the cell hinders rigorous quantitative analysis of CIZ1 patch incidence, estimation of the incidence of cells presenting a discrete CIZ1 focus revealed a high degree of variation amongst the different breast cancer cell lines (Figure 3.4B). While BT-474 and specially MDA-MB-231 cells exhibit a drastic loss in discrete CIZ1 patches, SKBR-3 cells are more likely to present a CIZ1 patch than the non-cancerous cell types. Once again, the remarkable similarity in percentage of cells presenting CIZ1 foci of MCF7 cells and non-cancer derived cells invites to reconsider the boundaries between culture-adapted or immortalised cells and low-grade tumour cell lines. Importantly, the low number of cells counted for some cell types (due to technical restrictions) together with the lack of independent repeats are limitations to be noted at the time to interpret this data.

These results revealed a highly altered CIZ1 localisation in all cell lines which appears to be more marked in high grade cancer cell lines. Notably, independent visualisation of CIZ1-RD and CIZ1-AD in the same cell reveals additional levels of corruption in the cancer cell lines.

## 5. Conclusions.

The results of this chapter suggest that the normal function of CIZ1 is compromised at some point in the process of culture adaptation or immortalisation of the cells even when it occurs in a non-cancerous fashion. Importantly, the highly variable incidence of CIZ1 foci in cancer cell lines together with the remarkable loss of CIZ1 domains colocalisation accumulations in the late stages of the disease evidence a profound dysregulation of the CIZ1 normal activity at the Xi during the tumorigenic transformation. One of the causes of the disruption of CIZ1 foci in culture-adapted and cancerous cells could be that morphological and epigenetic alterations of the Xi itself occurred during the transition of the cells to more proliferative states. Another cause could be an aberrant CIZ1 expression at either RNA and/or protein level. The complexity of the emerging picture suggests that both events could be simultaneously occurring. In order to investigate the relationship between cancer progression, CIZ1 foci disruption, and CIZ1 uncoupled domains, CIZ1 expression analysis becomes essential.



**Figure 4.1 (Heather Cook and Dawn Coverley, unpublished) Imbalanced CIZ1 domain expression in common solid tumours.** A) Top, representation of human CIZ1 exon structure and amplicons detected by quantitative RT-PCR tools. Probe sets are indicated in exons 5 and 6/7 (RD, pink and red), and exons 14/15 and 16/17 (AD, blue and green). Bottom, CIZ1 amplicon expression across 46 primary human lung tissue samples in Origene Array HLRT104, showing CT values for each of the four independent detection tool sets. B) Imbalanced CIZ1 domain expression in common solid tumours. Left, relative quantification (RQ) of CIZ1-RD (exon 7, white) and CIZ1-AD (exon 16, grey) in the indicated tumours sets in cDNA array CSRT101 (Origene), each containing nine independent tumours of increasing stage (left to right stages I to IV). Results were calibrated to an average of 3 unmatched control samples for each tissue type (C, identified individually as stage 0). Right, ratio of individual CIZ1-RD and CIZ1-AD RQ values, by stage, for the indicated tumour types, with quadratic regression trend line. Box indicates subset of tumours where CIZ1-RD levels exceed CIZ1-AD C) RQ after normalization to actin for CIZ1 RD (exon 7) and CIZ1 AD (exon 16) in primary breast tumour cDNA arrays BCRT103 and CSRT101 (Origene). Samples are ordered by clinical stage, where 0 represents histologically normal breast tissue. Box indicates subset of stage IV tumours where CIZ1-RD levels exceed CIZ1-AD.

## 2. Aims .

The aims in this chapter are to:

- i. Determine whether cell lines are a good model to develop functional analysis of ‘uncoupled expression’ by measuring the domain-specific relative expression levels of CIZ1 across the selected panel of breast cancer cell types grown in culture.
- ii. Examine the presence of quantitatively significant CIZ1 splice variants.
- iii. Investigate the relation between CIZ1 expression and the progressive disruption of CIZ1 localisation and enrichment at the Xi throughout the cell series.

## 3. Experimental design.

Ciz1 expression was analysed using two different approaches. CIZ1 domain-specific expression levels were analysed using quantitative RT-PCR (qPCR). CIZ1 levels and transcript diversity was analysed by Northern blot using domain-specific probes. To analyse the relative expression of CIZ1 transcripts detected by Northern probes, quantitative measurements based on signal intensity were performed.

## 4. Results.

### 4.1. CIZ1 expression is domain-balanced in all cell types and overrepresented in early stages of breast cancer.

In order to analyse CIZ1 domain expression, cDNA samples were generated from the total RNA of each cell type. CIZ1 RD and AD expression levels were measured independently by qPCR for each cell type (Figure 4.2A, B) using the same set of primers/amplicons from the previous study (Heather Cook and Dawn Coverley, unpublished). Relative expression levels were calculated using the  $2^{-\Delta CT} \times 100$  formula with GAPDH as gene of reference. This calculation method was preferred over the  $2^{-\Delta\Delta CT}$  method<sup>54</sup> because the first provides gene expression as a percentage of the expression level of the gene of reference, allowing for absolute quantitative comparisons between different qPCR analyses, while the second normalises an arbitrary sample expression as 1, reflecting only variations in gene expression relative to the selected sample.

In line with previous studies<sup>52</sup>, overall CIZ1 expression levels revealed an overrepresentation in cells belonging to the breast cancer molecular subtypes that correspond originally to less aggressive breast cancers, reaching almost 4-fold upregulation for BT-474 cells compared to HPMECs. Interestingly, a drastic reduction in CIZ1 expression could be observed in SKBR3 cells. Interestingly, the remarkable difference in CIZ1 expression levels in BT-474 and SKBR-3 cells inversely correlates with the incidence of CIZ1 foci in these cell lines (Figure 3.3B). This is consistent with a scenario in which elevated CIZ1 interferes with the normal CIZ1 accumulation at Xi<sup>65</sup>.

Consistently with the preliminary data (Heather Cook and Dawn Coverley, unpublished), CIZ1 also exhibited higher expression levels for CIZ1-AD in all breast cell lines analysed, revealing what appears to be an event of “uncoupled” CIZ1 domain expression. Interestingly, HPMECs also exhibited higher CIZ1-AD expression level, indicating that this “uncoupled” expression is not a cancer-specific situation.

A



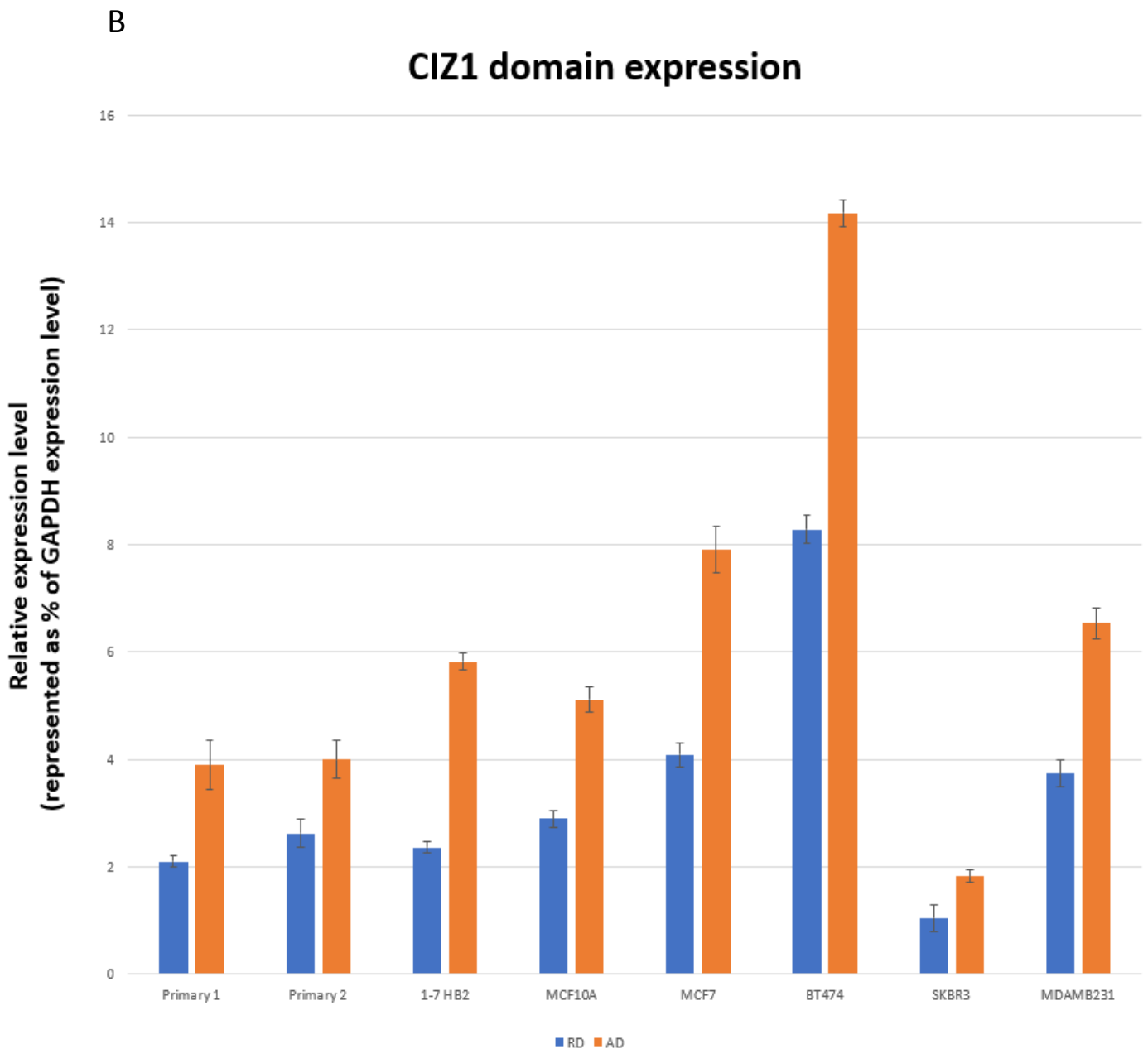


**Figure 4.2 CIZ1 domain expression is imbalanced is expressed and upregulated in early staged of the tumour.**

A) Representation of human CIZ1 transcript indicating translated (coloured) and untranslated (grey) exons. CIZ1 RD and AD are also indicated. Top, amplicons detected by qPCR are indicated in exons 6/7 (RD detection tool, blue) and exons 14/16 (AD detection tool, orange). Bottom, homology regions of the RNA-antisense probes used for Northern blot analysis (RD and AD, black). B) Expression levels of CIZ1 RD (blue bars) and CIZ1 AD (orange bars) in the indicated cell. Error bars represent standard deviation of 3 technical replicates. Expression levels are expressed as a percentage of GAPDH expression level for each indicated cell type.

#### 4.1.1. Technical considerations.

When independently analysed by qPCR, CIZ1 domain expression exhibited what appears to be an event of ‘uncoupled’ domain expression that occurs in all cells tested (Fig.4.1). Nevertheless, since the expression levels are inferred based on Ct value 22, and given the exponential nature

of the PCR, minor differences in primer efficiency could result in misleading differences in expression levels when absolute values are compared between reactions using different sets of primers. Moreover, when internally normalised to the expression levels of the same population of HPMECs, the difference in domain expression levels is drastically reduced (Fig. 4.3). For these reasons, primer efficiency tests are required in order to faithfully interpret this data. Another limitation to be noted at the time of interpreting this data is the fact that only technical repeats were performed, whilst independent repeats would valuably increase the statistical robustness of this analysis.

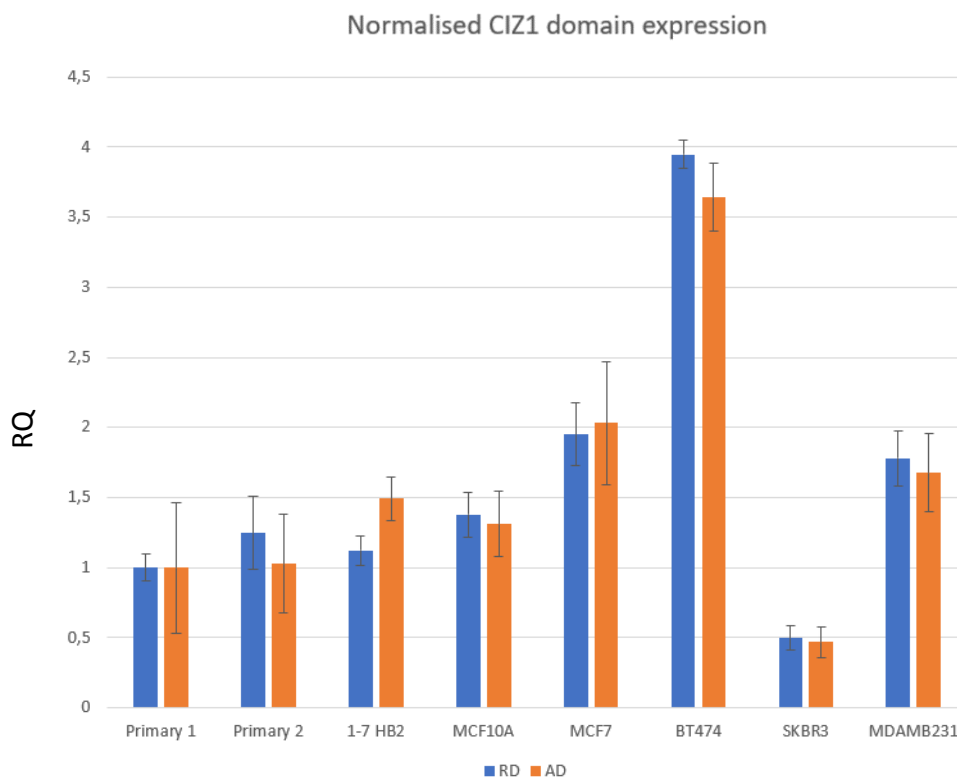
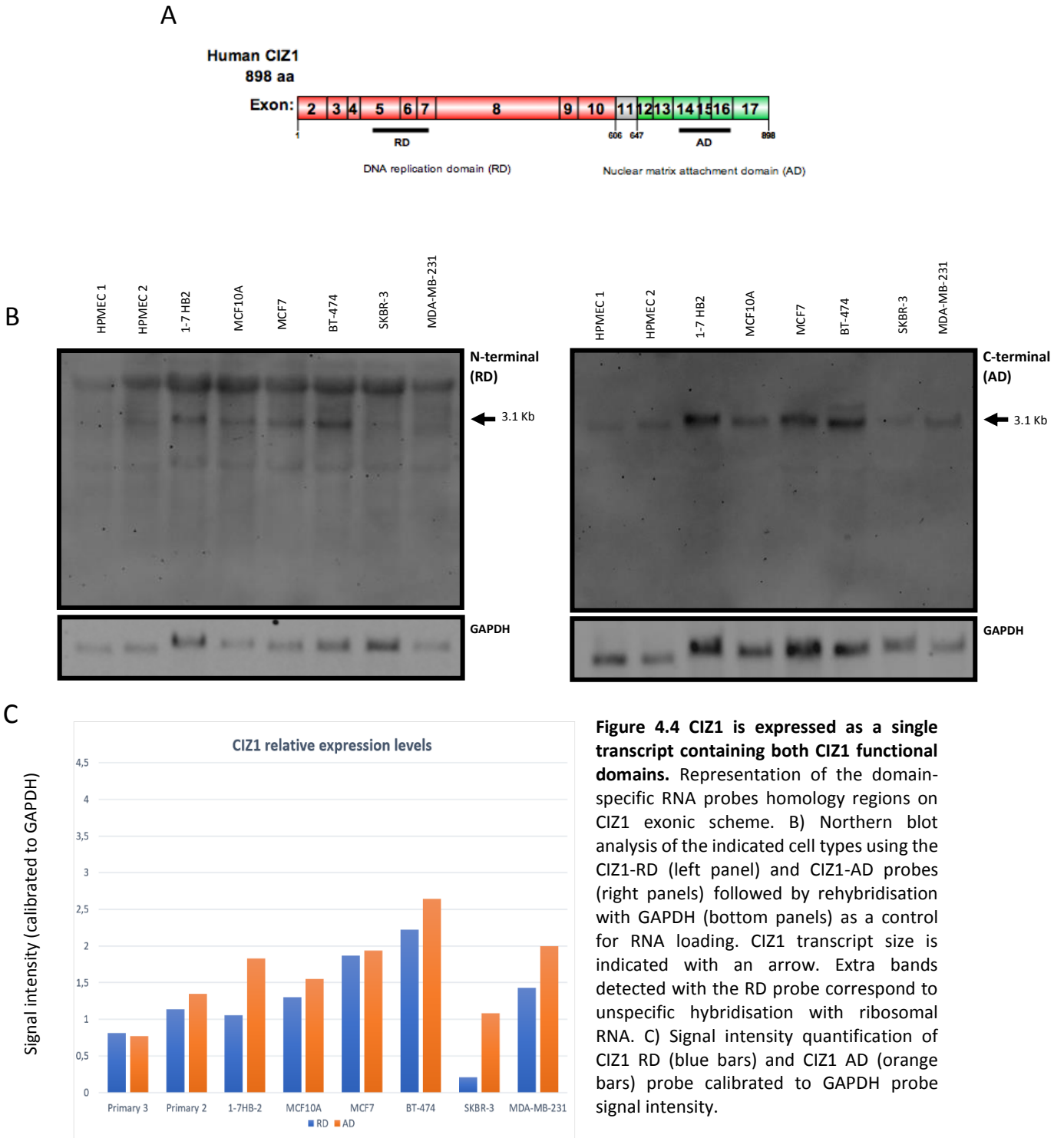


**Figure 4.3** CIZ1 domain expression levels normalised to the expression level of a population (Primary 1) of HPMECs using the formula  $2^{-\Delta\Delta Ct}$  54 .

## 4.2. No evidence of alternative transcripts.

The next step to investigate CIZ1 aberrant expression in breast cancer, was the analysis of CIZ1 splice variants by Northern blotting. Total RNA from each breast cancer and normal cell type was separated by electrophoresis and transferred onto a positively charged nylon membrane. CIZ1 mRNA was then detected using Digoxin-labelled RNA antisense probes with specific homology for CIZ1-RD and AD (Figure 4.4A). After at least two technical replicates per probe and several hybridisation conditions tested, a single 3.1 Kb transcript was detected with both probes,

consistent with full-length CIZ1 (~3Kb) (Figure 4.4B). Quantitative analyses based on signal intensity calibrated to the housekeeping gene GAPDH revealed that CIZ1 expression levels detected by Northern blotting are relatively consistent with the qPCR analysis (Figure 4.4C).



## 5. Conclusions.

Previous immunofluorescence analyses revealed a highly altered CIZ1 localisation in all breast cell lines. Moreover, CIZ1 domain colocalisation was heavily compromised in most of the cancer lines, where CIZ1 foci were more irregular and predominantly composed of CIZ1 AD. Here, transcript level expression analyses of CIZ1 domains using two different approaches consistently revealed an overexpression of CIZ1 in the breast cancer molecular subtypes that correspond with less aggressive breast cancers, suggesting that CIZ1 role in tumorigenesis could be of special relevance in the transition from normal breast cells to more proliferative states, whilst it might not be as relevant for the progression to more invasive stages. Interestingly, CIZ1 expression correlates inversely with CIZ1 foci incidence for BT-474 and SKBR-3 cells, suggesting that an excessively expressed CIZ1 could be altering its capacity to localise in a proper manner.

On the other hand, both analyses consistently showed higher CIZ1-AD expression levels across the whole cell series. Notably, although the difference in CIZ1 domain expression substantially varies between cell lines, the fact that this domain imbalance also occurs in both independent populations of HPMECs argues against the idea of CIZ1 uncoupled expression by itself as a contributing factor to the cancer development. Additionally, neither of the expression analyses revealed the inversion of CIZ1 RD/AD expression levels reported in the preliminary study of relative CIZ1 domain expression (Heather Cook and Dawn Coverley, unpublished), arguing against any correlation between cancer progression and CIZ1 domain expression imbalance.

Focusing on CIZ1 splice variant expression, Northern blotting revealed the presence of a single 3.1 Kb Ciz1 mRNA containing homology with Ciz1 RD and AD in all breast cell types tested, presumably full-length Ciz1 mRNA. Although more bands can be detected in with the CIZ1-RD probe, detailed analysis of size and shape (not shown) revealed that these extra bands consisted of unspecific hybridisation of the probe to ribosomal RNA. These results provide no evidence in support of alternative splicing in the breast cell types tested here. However, previous studies have reported relatively low abundance but physiologically relevant alternative Ciz1 messages linked with human pathologies<sup>35,52</sup>. These might be under the sensitivity threshold of the Northern blot assay, and not distinguished by the qRT-PCR used here. Increased total RNA load or poly-A pre-selection of the mRNA could be used to increase the sensitivity of the Northern blot assay in the future. Altogether, the results of this chapter suggest that transcript diversity is not preserved in cell lines. Nonetheless, post-translational modifications could result in the existence of different protein species containing independent CIZ1 domains, leading me to focus my attention on analysis of CIZ1 domains at the protein level.

## Chapter 5: Analysis of CIZ1 expression in breast cancer: Protein level.

---

### 1. Introduction.

It has been previously reported that when locally saturated, RNA-binding proteins and long non-coding RNAs can form assemblies that are in dynamic exchange with their environment (such as paraspeckles and stress granules), through a process known as ‘liquid–liquid phase separation’ (LLPS) <sup>66,67</sup>. When observed by high-resolution microscopy, the Xi presents about 100 Xist foci identifiable by RNA-FISH that are comparable in morphologies and dimensions to stress granules and paraspeckles <sup>26,68</sup>. Additionally, *Xist* protein network significantly overlaps with paraspeckles and stress granules components <sup>69</sup>, some of which have a role in Xist-mediated gene silencing <sup>70</sup> and recruitment of PRC proteins <sup>71</sup>. For these reasons, it has been proposed that phase separation might be driving XCI <sup>69</sup>.

In line with the previous literature <sup>31,65</sup>, the results of the chapter 3 of this study showed that CIZ1 localizes to the inactive Xi in HMECs. However, CIZ1 foci formation and CIZ1 domain-colocalisation is substantially altered in all breast cell lines tested. Analyses of CIZ1 transcripts described in chapter 4 revealed that CIZ1 domain expression is imbalanced and variably altered in all breast cell lines tested, but they fail to explain the relation between CIZ1 expression and CIZ1 foci disruption or cancer progression. A recent study analysed a cancer-specific CIZ1 truncated protein (CIZ1-F) that lacks the majority of CIZ1-AD, and correlated its expression with breast cancer grade <sup>52</sup>. A second data set, based on analysis of murine CIZ1 fragments (unpublished) suggests that some CIZ1 variants have the potency to act as dominant-negative controllers of other variants. The objective of this chapter is to analyse the variability of CIZ1 at protein level throughout the cell series, as well as investigating the properties of CIZ1-F and its capacity to disrupt endogenous assemblies.

## 2. Aims.

The aims in this chapter are to:

- i. Analyse the variability of CIZ1 domain expression at the protein level throughout the panel of cells.
- ii. Examine the differences in extractability of the CIZ1 species in breast cells.
- iii. Investigate the possible negative-dominant effect of CIZ1 fragments on endogenous CIZ1 to aggregates.

## 3. Experimental design.

CIZ1 domain expression at protein level was analysed by Western blot using total protein lysates and domain-specific antibodies. Immunofluorescence detection of CIZ1 domains combined with serial nuclear extraction assays were performed in order to characterise the variations in CIZ1 extractability. Expression levels of CIZ1-F across the series of cells were analysed by qPCR. To examine the effect of CIZ1 fragments on endogenous CIZ1, 1-7HB2 cells were transfected with CIZ1-F or CIZ1-N57 (explained below) and endogenous CIZ1 signal was compared with non-transfected cells.

## 4. Results.

### 4.1. High diversity of CIZ1 species and domain-specific fragments in normal and cancer cells.

To investigate the degree of heterogeneity of CIZ1 expression at the protein level, Western blot analyses were performed in total cell lysates of two independent populations of HPMECs and breast cell lines. A preliminary analysis using antibodies raised against a peptide that encompasses the majority of the CIZ1-AD (Figure 5.1A) revealed at least 3 different CIZ1 forms consistently expressed by both populations of HPMECs (Fig. 5.1B, top panel). In contrast, cancer cell lines exhibited a higher diversity of CIZ1-AD fragments where each cell type presented a

different expression pattern. Interestingly, the normal cell line MCF10A expressed CIZ1 species that were in common with both cancer and HPMECs. These results suggest that while CIZ1-AD *basal* protein expression is more diverse than originally expected, it appears to degenerate in the tumour cell panel, presenting cancer-specific species that vary depending on the cancer line. In line with this, further analyses using antibodies against a more defined epitope of CIZ1-AD also revealed a 140 KDa cancer-specific form that was not detectable in neither HPMECs nor MFC10A cells (Fig. 5.1B, middle panel). 1-7HB2 cells were not included in this preliminary study because it was performed prior to the incorporation of the cell line to the cell series.

Unfortunately, protein loading determined by Histone H3 detection revealed almost undetectable protein levels for HPMECs in the preliminary analysis. For this reason, subsequent efforts focused on several attempts at protein load equalising, all of them resulting in unsuccessfully imbalanced protein load when examined by detection of either Histone H3 or the helicase MCM2 (BM28, Fig. 5.1C). The relative abundance of some CIZ1 species expressed by HPMECs with respect to the rest of the cell lines and the intensity of the unspecific signal in the background of the lanes suggest that the protein load is considerably more even than what the loading controls revealed. In any case, the detection of other abundant and constitutively expressed proteins such as actin or tubulin, as well as protein assays based on colorimetric measurements (including Bradford, Lowry or BCA assays) are alternatives that could be used next. Nevertheless, it is important to remark that I did not succeed in finding suitable loading control for the HPMECs during the time of this study. For this reason, I refrained from making any quantitative comparison of CIZ1 domain expression at the protein level between HPMECs and the breast cell lines. Once this has been stated, I proceed to the next step of the protein analysis focusing on the qualitative aspects of CIZ1 protein expression.

Based on the high diversity of CIZ1-AD forms detected in the preliminary analysis, I opted for an antibody that recognises a defined epitope at the 7/8 exon junction in order to analyse CIZ1-RD protein expression (Fig 5.1A). In line with the previous result, CIZ1-RD expression was consistent among both HPMECs populations and the non-cancerous breast cell lines (including 1-7HB2 cells) where a 40KDa form was substantially the most abundant specie (Fig 5.1D). Interestingly, this form is lost in the first three breast cancer molecular subtypes, only detectable in MDA MB 231 cells, which represents the most aggressive and metastatic breast cancer subtype. This result supports the idea that a perturbed CIZ1 biology is more relevant in the development of less aggressive breast cancers. Remarkably, only a 68 KDa species was detectable via epitopes in both CIZ1 domains in HPMECs, (Fig. 5.1E, asterisk), being the most abundant CIZ1 forms only detectable via epitopes in either CIZ1-RD or AD.

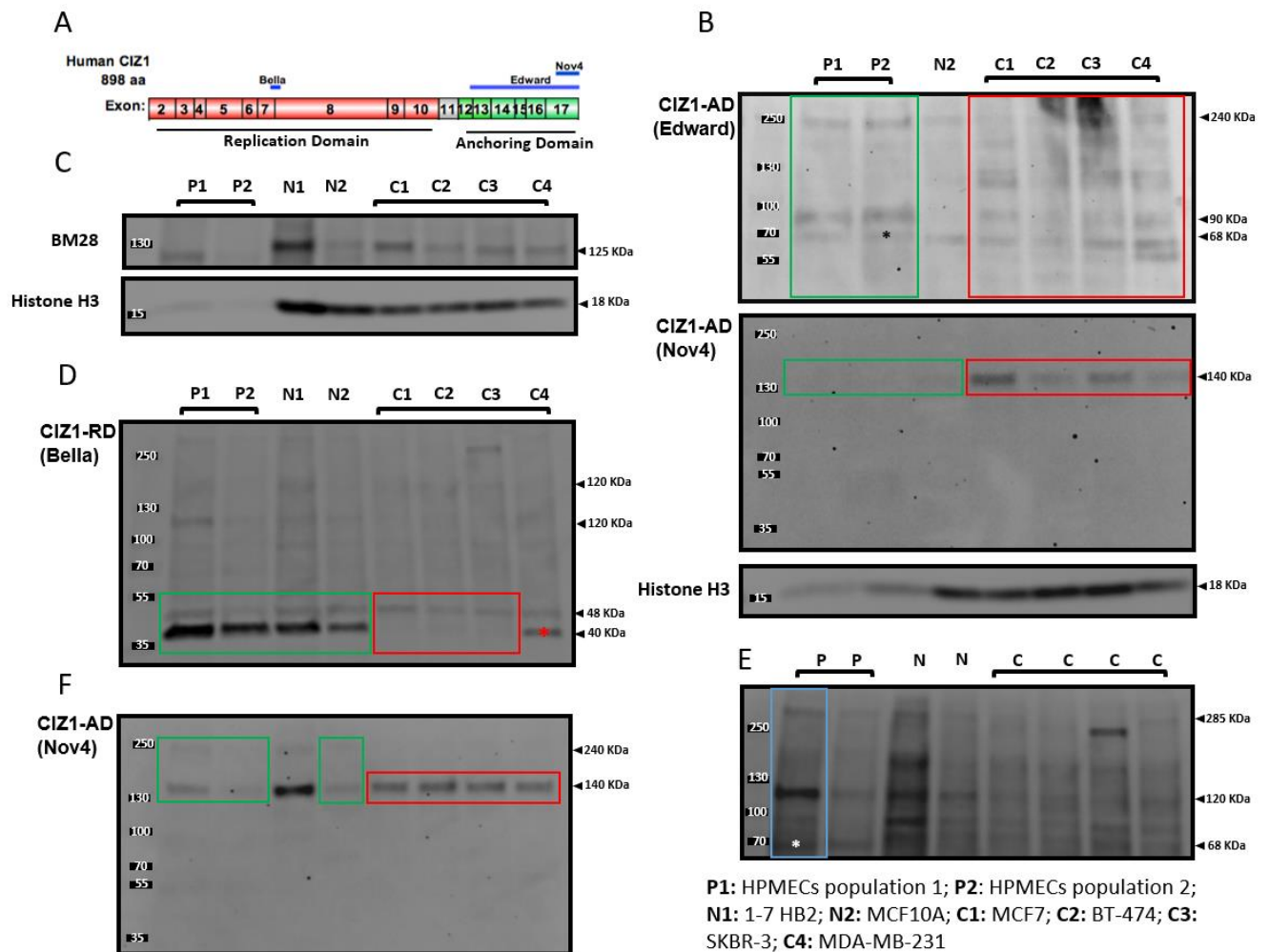


**Figure 5.1 CIZ1 protein expression is highly complex and exhibit normal/cancer patterns.** A) Representation of CIZ1 exonic and domain structure. Different antibodies used for western blot assays are indicated. B) Top panel: Preliminary CIZ1-AD expression analyses revealing consistent expression patterns for independent populations of HPMECs (P, green box) that is partially conserved normal cells (N) and disrupted in cancer cells (C, red box). Middle panel: Detection of cancer specific 140KDa CIZ1 form. Bottom panel: Loading control reveals a dramatically uneven protein load. The relatively equal abundance of CIZ1-AD detected in top panel rises concerns about the validity of this loading control. C) Different attempts failed to balance protein load when analysed by Histone 3 or BM28 detection. D) Western blot using anti-CIZ1-RD antibodies revealed a dominant 40KDa form overrepresented in HPMECs and normal cells (green box) that is lost in the first three stages of breast cancer (red box) and regained in the last stage (red asterisk). E) Longer exposure times of CIZ-RD detection revealing unspecific background signal in all lane as an indirect protein loading control reveal relatively even protein load for HPMECs (blue box). Only a 68KDa form can be detected in HPMECs using antibodies against both domains independently (Asterisk). F) Maximum protein load possible for HPMECs and MCF10A cells revealed the presence of the 140KDa although in much lower concentrations than cancer cell lines. Unexpectedly, 1-7 HB2 cells exhibited the highest expression of this form.

A second analysis of CIZ1-AD expression with a higher protein load for HPMECs and including 1-7HB2 cells revealed that the 140KDa form preliminarily identified as cancer-specific (Fig. 5.1 B) is also expressed in HPMECs although in much lower levels (Fig. 5.1F). Surprisingly, 1-7HB2

presented the highest levels of expression of this form, rising concerns again about suitability of the current non-cancer breast cell lines as a model for breast “normal” state.

Altogether, the results of these analyses revealed that CIZ1 expression is highly intricate even at its *basal* state in normal cells, and appears to exhibit a physiological event of independent domain expression. However, the fact that it is consistent in both independent HPMECs populations and shares many features with the non-cancer cell lines brings the hope that CIZ1 *basal* expression will eventually be interpretable, though further investigation is required.

Previously available information about the origin and specificity of the antibodies used in these protein analyses are specified in Chapter 2 (Table 2.7). Preliminary results in the validation of the specificity of these antibodies and further discussion can be found in the Appendix (Fig. A2).

#### **4.2. Cancer-specific CIZ1 fragments interact with the nuclear matrix in an RNA-independent fashion.**

The next step in the characterisation of the highly diverse CIZ1 species present in breast cells was to monitor CIZ1 localisation throughout a series of washes that sequentially remove different fractions of the nuclear components of HPMC, 1-7 HB2, MCF7 and MDA-MB-231 cells (Serial nuclear extraction, Fig. 5.2A).

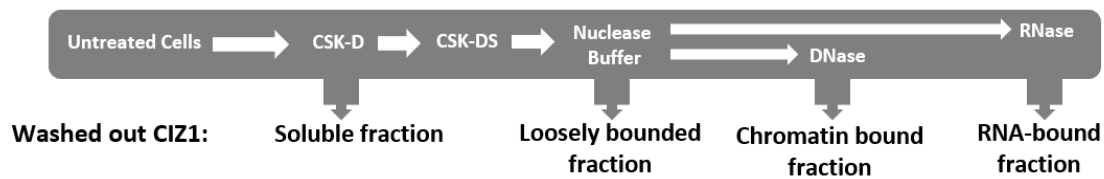
When washed with highly-saline (500mM) detergent buffer (CSK-DS), HPMCs and 1-7 HB2 cells revealed a substantial loss of the CIZ1-RD signal compared to cells treated only with detergent buffer (Fig. 5.2B). CIZ1 foci were also significantly more dispersed throughout the nucleus although both CIZ1 domains could be found within it and mostly colocalised. In contrast, cancer cells retained higher levels of CIZ1-RD and clearly exhibited independent CIZ1 domains occupying distinctively different locations. These results support the idea that while a significant fraction of CIZ1-RD is loosely bound to different nuclear proteins in non-cancerous cells, the presence of cancer-specific CIZ1 fragments in cancer cells might be altering these interactions and promoting aberrant aggregation.

Next, cells were washed in DNase-containing CSK buffer prior to fixation (Fig. 5.2C). All DNase treated cells exhibited an increase in CIZ1 signal for both domains as previously reported<sup>53</sup>. This suggests that the remaining CIZ1 unmasked by DNA removal is interacting with the nuclear matrix in a chromatin-independent fashion. Interestingly, while chromatin removal also revealed in some cells what appeared to be CIZ1 foci, these CIZ1 aggregations were predominantly composed of CIZ1-RD in contrast with the normal CIZ1-AD dominated foci. These

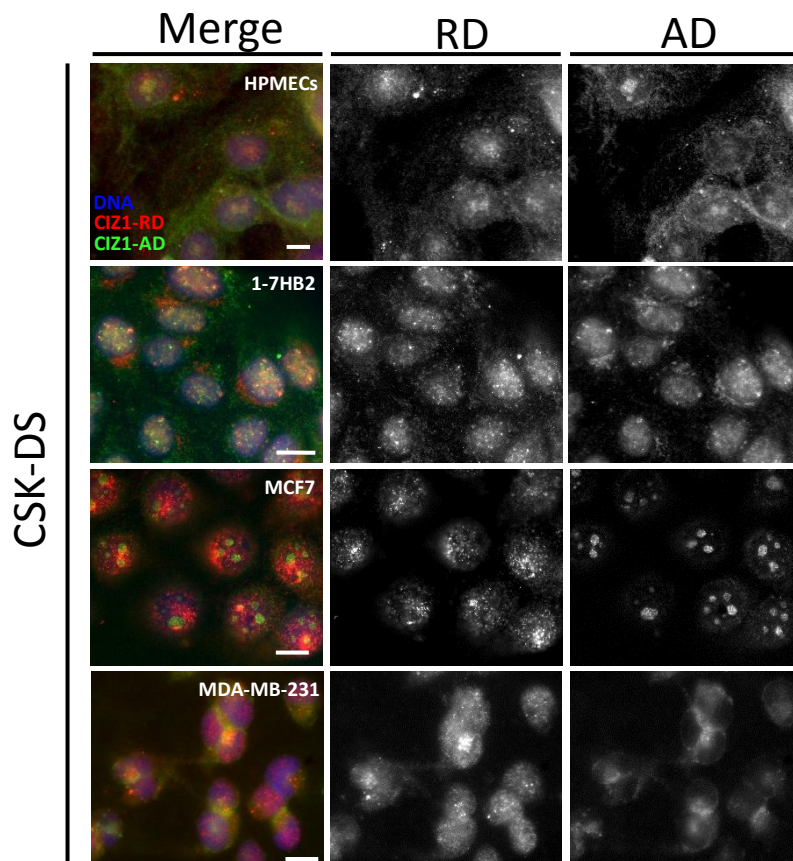
results suggest that while CIZ1-RD interactions are chromatin-independent, CIZ1-AD might require chromatin structures to aggregate.

Parallely, cells were washed in RNase-containing CSK buffer (Fig. 5.2D). As previously reported for murine 3T3 cells and PEFs <sup>57</sup>, RNase digestion promoted the removal of both CIZ1 domains in HPMECs and 1-7HB2 cells (Fig. 52C). Remarkably, CIZ1-RD remained clearly present in the nucleus of MCF7 cells. Similarly, MDA-MB-231 conserved both CIZ1 domains under RNase treatment although they did not completely colocalise. These results evidence the presence of CIZ1 fragments that interact with the nuclear components of the cancer cells in a very different way than reported in previous literature about 'normal' CIZ1 <sup>31,57</sup>. The fact that some CIZ1 fragments remained under all extraction conditions in cancer cells is not in contradiction with the idea of aberrantly expressed cancer-specific CIZ1 fragments that might be altering CIZ1 normal localisation in a dominant-negative way.

A



B



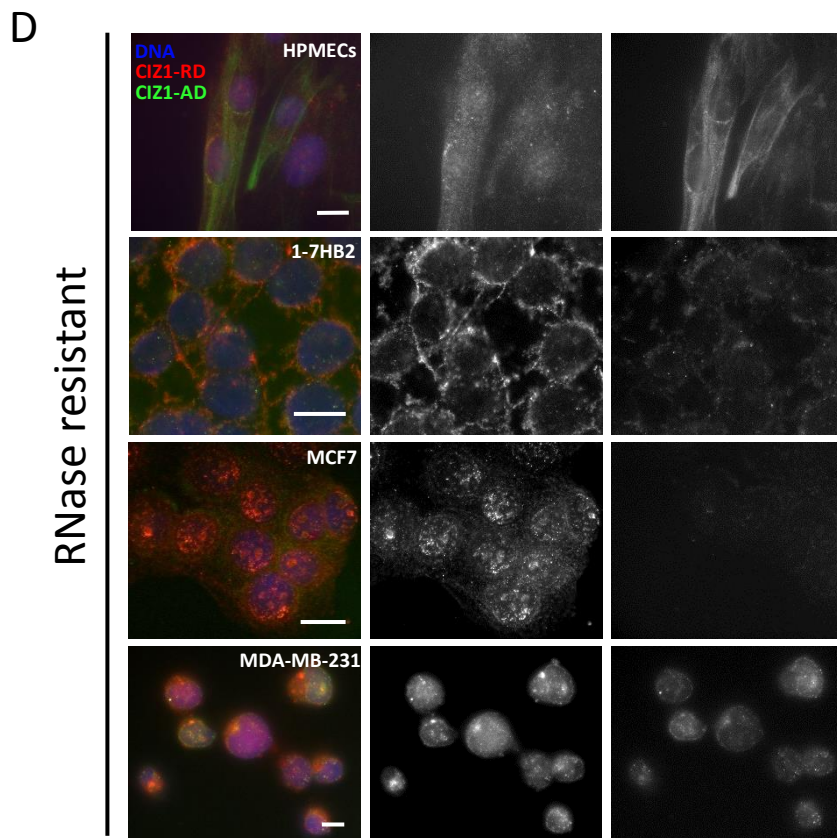
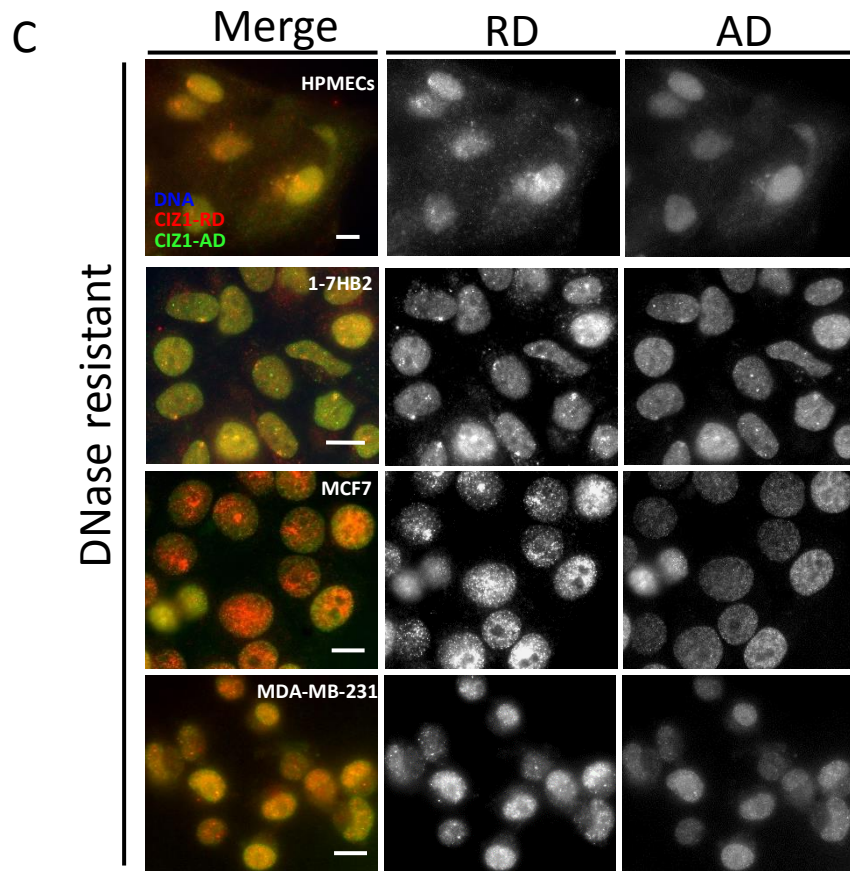


**Figure 5.2 Serial matrix extractions revealed aberrant CIZ1 extractability profiles in cancer cells.** A) Schematic representation of the sequential extraction of different nuclear components. B) Immunolocalisation of CIZ1-RD (red) and CIZ1-AD (green) using the same antibodies of previous immunofluorescence analyses (Fig. 3.3A) in CSK-DS treated cells. Scale bars represent 10 microns. C) Immunolocalisation of CIZ1-RD and CIZ1-AD after DNA removal and CSK-DS wash to remove nucleotides and DNA fragments. D) Immunolocalisation of CIZ1-RD and CIZ1-AD after RNA removal and wash to remove ribonucleotides and RNA fragments.

A full nuclear matrix extraction utilising a mock buffer instead of primary antibody was performed in MDA MB 231 cells as a negative control (Appendix, Fig. A1).

### 4.3. CIZ1-F is not expressed in HPMECs and affects endogenous CIZ1 aggregation in 1-7HB2 cells.

In order to investigate the capacity of CIZ1 cancer-associated fragments to interfere with CIZ1 normal localisation, I opted for using CIZ1-F, a naturally occurring truncated version of CIZ1 that lacks the majority of the AD, and that is overrepresented in early stage common solid tumours<sup>52,24</sup> (Fig.5.3A). Firstly, CIZ1-F expression levels were analysed across the cell series by qPCR (Fig. 5.3B). All breast cell lines exhibited variable levels of CIZ1-F, though in line with published work, they were several orders of magnitude lower than CIZ1 RD and AD domain expression levels previously analysed. Interestingly, no detectable levels of CIZ1-F transcript were found in either of the HPMECs independent population tested. This result supports the idea of CIZ1 cancer-specific variants, and suggests that such alterations in CIZ1 normal expression could be of special relevance in highly proliferative cells, even in relatively low-aggressiveness breast cancer subtypes or in non-cancerous events of cellular immortalisation.

The next step was to test the biological relevance of these CIZ1 variants in altering CIZ1 normal function by transfecting 'normal' breast cells with different GFP-CIZ1 constructs and monitoring changes in endogenous CIZ1 signal (Fig. 5.3B). Given that HPMECs are challenging to culture and transfer I initiated this work with 1-7 HB2 cells. Cells were transfected with a plasmid containing either CIZ1-F<sup>52</sup> or N-57, a CIZ1-RD construct that express almost exclusively the Poly-Q region proximal to the N-terminal of murine CIZ1 (generated by Susie Holliman undergraduate project 2018/19). Due to the irregularity of CIZ1 foci exhibited in breast cell lines, and in order to perform an unbiased analysis, endogenous CIZ1 signal was measured in transfected and untransfected cells based on image pixel intensity (Fig. 5.4A). Although mean pixel intensity across the nucleus was significantly reduced in cells transfected with either CIZ1-F or N-57, the disruptive effect of transfected CIZ1 fragments is more pronounced when comparing maximum

pixel intensity (Fig. 5.3B). This result suggests that CIZ1 fragments interfere with CIZ1 normal capacity to form aggregates in breast cells. This experiment was performed analysing multiple pictures from two technical repeats. For this reason, performing independent biological repeats would be important in order to support these results.

A

Human CIZ1 transcript:



CIZ1-F transcript:



B

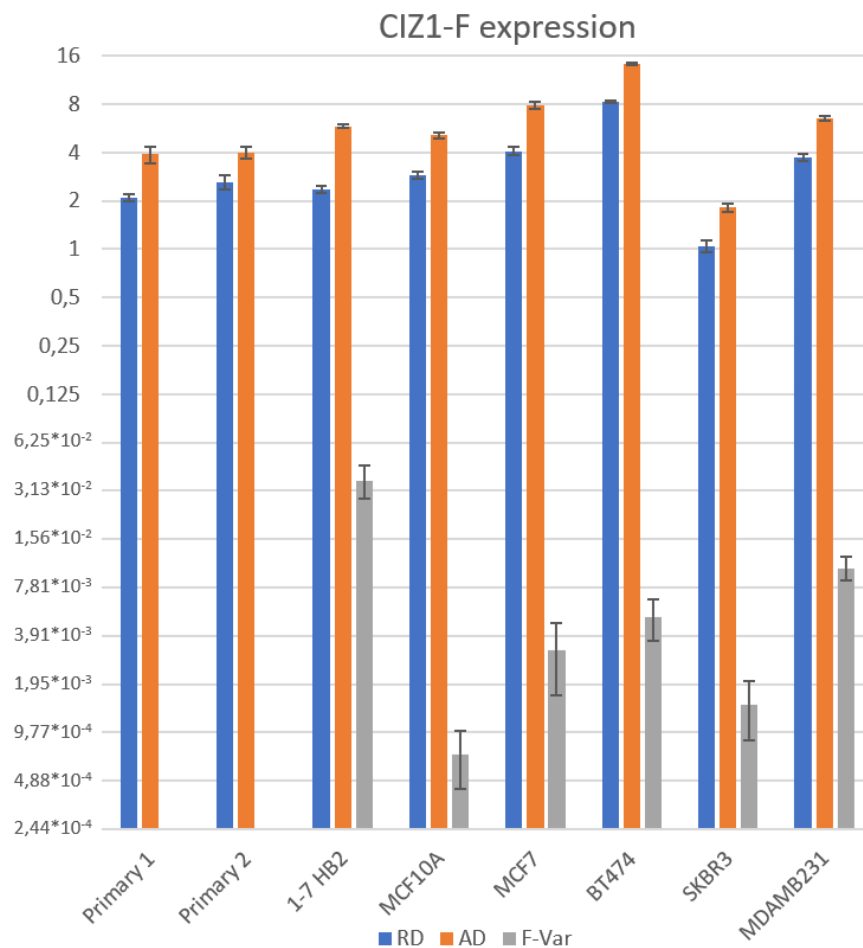
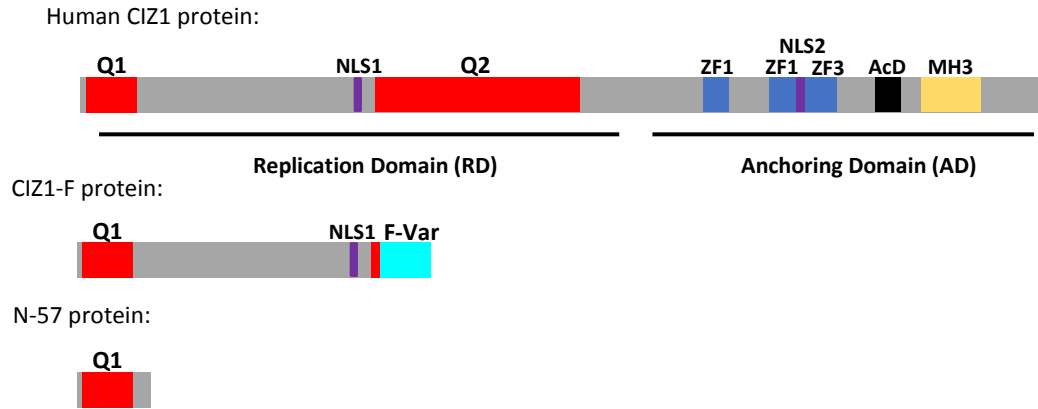
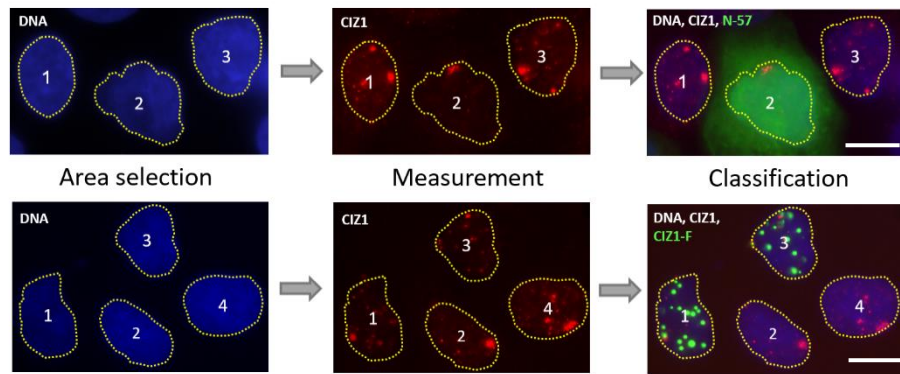


**Figure 5.3 CIZ1-F is variably expressed by breast cell lines but not HPMECs.** A) Scheme of human CIZ1 and CIZ1-F transcripts indicating untranslated (grey) and translated (green and blue) exons. Primers used for CIZ1-F expression levels analyses are indicated in red. Premature stop codon is indicated in exon 13. B) CIZ-1 expression levels measured by qPCR (grey) revealed variable levels of expression in different cell lines. Neither of the independent HPMEC populations (Primary 1 and 2) expressed detectable CIZ1-F levels although they expressed similar GAPDH levels than the rest of cell lines. Expression levels are indicated in logarithmic scale to be comparable with normal CIZ1 domain expression.

A



B



C

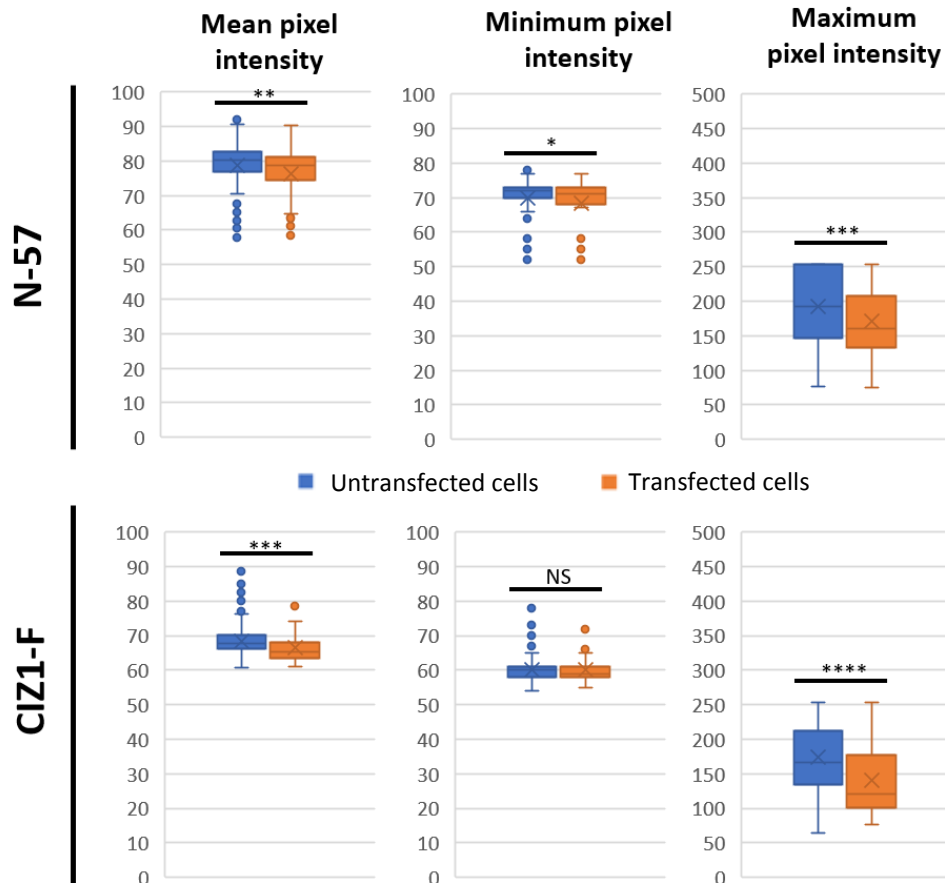


**Figure 5.4 CIZ1-F and N-57 significantly affect endogenous CIZ1 capacity to aggregate.** A) Representation of human CIZ1, CIZ1-F and N-57 domain structure. Q: Glutamine-rich domain, NLS: Nuclear localisation sequence. ZF: Zinc finger. AcD: Acidic domain. MH3: Matrin 3 homology domain. F-var: CIZ1-F specific sequence, encoded by an alternative reading frame with a premature stop codon in exon 13. B) Scheme of the systematic analysis of endogenous CIZ1 signal based on pixel intensity. Nucleus area was defined based on DNA stain. Pixel intensity was measured exclusively for endogenous CIZ1 by measuring red fluorescence. For an unbiased study, all cells in each field were measured and then retrospectively classified as transfected/untransfected based on fluorescence in the green channel. C) Cells transfected with N-57 showed significantly reduced minimum, mean and maximum pixel intensity values. Cells transfected with CIZ1-F only exhibited a significant decrease in mean and maximum pixel intensity. Asterisks represent statistically significant differences between pixel intensity of transfected and untransfected cells (NS= No significance; \* = p value  $\leq$  0.05; \*\* = p value  $\leq$  0.01; \*\*\* = p value  $\leq$  0.001; \*\*\*\* = p value  $\leq$  0.0001). Scale bars represent 10 microns.

## 5. Conclusions.

In summary, the results of this CIZ1 protein expression analysis revealed an intricate picture, even in the primary state of the breast cells, so that solid conclusions cannot be drawn from it. Nevertheless, the consistency between CIZ1 expression of independent HPMECs and the disruption of this pattern in cancer cells points out that CIZ1 expression is specifically altered in tumorigenic events and further investigation could result in the unravelling of the complexity of CIZ1 protein expression. For instance, the 40KDa dominant species detected only in HPMECs and non-cancerous cell lines could be a candidate to account for the massive loss of CIZ1-RD signal in high-salt treated HPMECs and normal cells. Serial nuclear extraction analyses also revealed a highly complex scenario. The fact that predominantly CIZ1-RD signal was detectable after all sequential extraction steps in cancer cell nuclei suggests that the PolyQ regions present in CIZ1 N-terminal might be relevant for its aberrant interactions with the nuclear components. In light of these results, I decided to utilise CIZ1-F and N-57 to investigate a potential dominant-negative effect of PolyQ-rich CIZ1 fragments in CIZ1 normal localisation. The preliminary expression analysis revealed remarkably low CIZ1-F expression levels that are under the sensitivity threshold of the previous northern blot analyses, opening the possibility of more undetected alternative CIZ1 variants that might be biologically significant. Transfection of both CIZ1-F and N-57 constructs in 1-7 HB2 cells resulted in significantly decreased endogenous CIZ1 signal, suggesting that the overexpression of PolyQ-rich CIZ1 fragments might be affecting CIZ1 normal aggregation in a dominant-negative fashion. This idea of endogenous CIZ1 foci disruption is supported by the fact that while the minimum pixel intensity was less or not significantly affected, the mean and maximum pixel intensity exhibited highly significant alterations. Further investigation comparing chromatin modification status or gene expression between transfected and untransfected cells would contribute to elucidate the impact of these CIZ1 fragments in the breast cell biology.

## Chapter 6: Discussion

---

There is a growing number of studies that link CIZ1 with devastating human pathologies ranging from neurological malignancies such as Alzheimer's<sup>35</sup> disease or muscular dystonia<sup>33,34</sup> to most common solid tumours, including liver<sup>42,59</sup>, lung<sup>36,58</sup> and breast cancer<sup>23,38</sup>. For this reason, understanding CIZ1 function becomes essential to elucidate the contribution of CIZ1 aberrant expression to the development of these pathologies. Previous studies focused on CIZ1 capacity to promote mammalian DNA replication<sup>21</sup> by coordinating spatially and temporally the concerted activities of cyclins E and A<sup>20,72</sup>. This replication activity together with the implication that CIZ1 may be linked to the DNA damage checkpoint via p21<sup>Cip1</sup> direct interaction<sup>5</sup> represent links with central molecular mechanisms that could be underpinning CIZ1 relevance in proliferation, invasiveness and anchorage-independent growth of cancer cell lines in vitro<sup>36-46</sup>. However, recent studies implicating CIZ1 in *Xist* anchoring<sup>57</sup> and maintenance of the epigenetic status of the Xi<sup>31</sup> broadens the spectrum of mechanisms through which CIZ1 aberrant activity could be contributing to cancer development. A correlation between aberrant Xi inactivation and cancer has been previously reported<sup>49</sup>. In particular, aberrant nuclear organization and loss of canonical epigenetic repressive marks of the Xi are hallmarks of breast cancer<sup>47</sup>. Previous studies have reported *Xist* misbehaviour in breast cancer cells, though they focused on the relation between the breast cancer predisposing gene BRCA1 and *Xist*<sup>73</sup>. Therefore, to the best of my knowledge this is the first study that explores the implications of CIZ1 aberrant expression in breast cancer development, using its role in the Xi as a model. Conveniently, all breast cells utilised in this study are reported to be wild-type for the gene BRCA1 (Table 2.1), theoretically eliminating any potential interference of this gene with *Xist* biology.

Consistent with a role for CIZ1 at the Xi previously reported in PEFs<sup>57,31</sup>, immunodetection of CIZ1 revealed a single discrete accumulation of both CIZ1 RA and AD domains, that colocalises with Xi markers<sup>29</sup> within the nucleus of all HPMECs (Fig.3.2, Fig.3.3). As might be expected, breast cancer cells exhibited highly disrupted CIZ1 localisation where CIZ1 foci were more irregular or inexistent, and domain colocalisation was heavily compromised (Fig.3.4). Notably, CIZ1 foci features were already substantially compromised in non-cancerous cells in long term culture. This result is in line with previous studies reporting similar effects of culture-adaptation and CIZ1 deletion in PRC1/2 activity and gene expression<sup>31</sup>, and suggests that CIZ1 normal activity is compromised in the very early steps of a cells transformation towards a culture-compatible proliferative state.

In general, this defect in CIZ1 capacity to aggregate at the Xi could be influenced by alterations in either CIZ1 expression or Xi integrity, at the level of *Xist* or some unknown intermediary factor. There are different studies that have reported alterations in CIZ1 expression affecting its subnuclear localisation such as the cancer-associated missplicing of exon 4<sup>51</sup> or the alternatively spliced exon 8 linked with Alzheimer's disease<sup>35</sup>. Since it is currently under discussion whether the aberrant features observed in the Xi of breast cancer cells is caused by epigenetic instability or genetic loss<sup>47</sup>, I decided to focus on the analysis of CIZ1 transcript and protein expression in cells derived from different stages of breast cancer development. A comparative analysis of Xi chromatin status, genetic integrity and gene expression across the breast cell series would be of central value for future investigation, and pave the way for direct analysis of tumour specimens. It is also worth noting that further research should also analyse real tumour samples in order to account for the natural heterogeneity and complexity of the breast cancer biology.

One of the mechanisms that might be underpinning the link between CIZ1 aberrant expression and a corrupt Xi epigenetic status is the presence of CIZ1 fragments containing only some of its functional domains. Thus, CIZ1-AD fragments containing RNA-binding motifs, but lacking protein-protein interaction capacity could be saturating *Xist* anchoring points, and preventing it from recruiting other proteins relevant for Xi epigenetic maintenance or even localising to the Xi. Alternatively, CIZ1 RD fragments containing excessively promiscuous protein-protein interaction domains but lacking RNA-binding capacity could lose its normal localisation at the NM and the Xi. Thus, more ubiquitous CIZ1 fragments that also interact more tightly with the nuclear matrix components, could represent foci of enhanced replication CDK activity that could lead to the onset of the early stages of cancer. For this reason, a high variety of CIZ1 species, or events of independent CIZ1 domain expression might be expected in the analysis of CIZ1 expression in cancer.

Unexpectedly, northern blot analyses only detected a single transcript consistent with full-length CIZ1 for all breast cells tested (Fig.4.4). I did not see evidence of smaller transcripts, though it should be noted that several studies have reported biologically significant CIZ1 variants<sup>35,51,52</sup> with relative expression levels far below the expected sensitivity threshold of the northern blots used in this study. One way to identify the sensitivity limit of this northern setting could be to estimate the copy number of CIZ1-RD and AD mRNA per ng of total RNA of a sample by qPCR utilising absolute quantification methods<sup>74</sup>, and then performing a northern blot assay

loading decreasing amounts of total RNA until reaching the minimum load (hence minimum CIZ1 mRNA copy number) at which CIZ1 probe hybridisation is detectable.

On the other hand, to explore the possibility of these smaller transcripts, I would need to pre-select mRNA or increase total RNA load to improve sensitivity. However, the challenging culturing conditions and limited availability of HPMECs prevented me from embarking on this analysis during the time available. However, future efforts could lead to the identification of new relevant cancer-specific CIZ1 transcripts for which PCR-based detection has not been developed yet. Altogether, this body of findings supports that the high CIZ1 expression variability observed by immunofluorescence analyses is derived mainly from protein level variation.

Supporting the idea that considerable CIZ1 variation occurs at the protein level, western blot analyses with a set of anti-CIZ1 antibodies revealed an intricate CIZ1 protein expression pattern, where high diversity of CIZ1 species could be detected even in HPMECs (Fig.5.1). Despite the complexity of the emerging picture, these analyses provided some valuable insights about CIZ1 protein expression, such as the existence of diverse CIZ1 domain-specific fragments consistently expressed in HPMECs. Moreover, I have documented the over-representation of some species in cancer cells, and the absence of species that are dominant in primary cells at the early stages of breast cancer. Altogether, although physiological CIZ1 protein expression is more complicated than initially expected, consistent alterations in CIZ1 expression patterns are observed in breast normal cells compared to cancer cells, promising that we will eventually be able to describe a discernible scenario. It is worth noting that data generated by others in the Coverley lab have recently generated evidence for stable oligomerisation of purified recombinant human and mouse CIZ1 that persist in SDS-PAGE (G. Turvey and S. Sofi, unpublished), which might underpin some of the complexity that I have observed in cellular lysates.

In any case, after these analyses it is clear that multiple CIZ1 fragments exist in breast cells. Moreover, serial nuclear extraction assays revealed different behaviours of these CIZ1 fragments in normal and cancer cells (Fig.5.2; 5.3). The existence of cancer-specific CIZ1 populations resistant to all extraction steps evidence that CIZ1 normal biology is highly altered at the level of its capacity to assembly with nuclear component. The fact that CIZ1-RD is the predominant form remaining within the nucleus of cancer cells after the serial extraction suggests that the glutamine-rich domains contained in this CIZ1 fragments could be playing an essential role in this aberrant aggregation dynamic. Again, work from others in this lab has shown that the polyglutamine domain of CIZ1 is required for it to be targeted to Xi (C. Scoynes and S. Holliman, unpublished). A growing number of studies are beginning to explore the

implications of LLPS events in the XCI<sup>69</sup>. *Xist* protein network is highly enriched in glutamine-rich RNA-binding proteins including CIZ1<sup>26,68</sup>, which are known to be the main drivers of LLPS<sup>66,67</sup>. Dominant-negative effect of glutamine-rich mutant proteins in normal protein aggregation with devastating biological implications have been extensively reported<sup>75,76</sup>. In line with this, normal breast cells transfected with CIZ1 glutamine-rich fragments that are highly suitable for aberrant aggregation presented significant alterations in endogenous CIZ1 assembly (Fig. 5.4). Importantly, the impact of the cancer-associated variant CIZ1-F<sup>52</sup> in normal CIZ1 biology represent a solid evidence of the capacity of aberrant CIZ1 fragments for interfering with physiologically relevant protein aggregation events, and more research in this line is required in order to unravel the increasingly complex CIZ1 protein interaction network.

In summary, this study has opened an exciting new approach towards the study of CIZ1 contribution to breast cancer development. Although the analyses of CIZ1 expression in breast cells evidenced a highly complex scenario, this study has provided some insights of what might be one of the main molecular mechanisms underpinning the role aberrant CIZ1 expression in human disease.

## Appendix

### 1. CIZ1 implication in Human Pathology: Bibliographic summary.

**Table A.2 Exhaustive summary of studies implicating CIZ1 in human disease.**

<b>Neuromuscular disorders</b>	<b>Results</b>	<b>Methods</b>
<b>Blepharospasm: A genetic screening study in 132 patients (Hammer M, et al., 2019).</b>	- 20 variants of CIZ1 in blepharospasm patients, most of them benign.	-Sanger Sequencing
<b>Mutations in CIZ1 cause adult onset primary cervical dystonia (Xiao J, et al., 2012).</b>	- Disruption of 3 exonic splicing enhancer mutation in exon 7 of CIZ1 in CD patients.	-Whole exome sequencing
<b>Cancer</b>	<b>Results</b>	<b>Methods</b>
<b>CIZ1 Expression Is Upregulated in Hemangioma of the Tongue (Wang Y, et al., 2018).</b>	-Overexpression in benign cancer -Knockdown inhibits migr. and prol. In vivo	-IC -Western blot -Migration assays
<b>CIZ1-F, an alternatively spliced variant of the DNA replication protein CIZ1 with distinct expression and localisation, is overrepresented in early stage common solid tumours (Swarts DRA, et al., 2018).</b>	- Deletion of part of the exons 8 and 12, and all of exons 9-11 in mRNA. Frame-shift causes premature stop in exon 13. - Overrepresented in Breast and colon Cancer, mostly in early stages. - Similar extraction to CIZ1 profile but not on Xi.	- Exon-junction array - IF and NM extraction - qPCR
<b>Examining transcriptional changes to DNA replication and repair factors over uveal melanoma subtypes (Kucherlapati M., 2018).</b>	- CIZ1 exon 4 skipping evidences - CIZ1 Intron 3 contains a mononucleotide repeat previously mechanistically associated with exon 4 skipping - Almost all tumours and normal samples had some CIZ1 alteration.	- Whole exome sequencing - Whole genome sequencing - mRNA, miRNA and lncRNA expression analysis - DNA methylation analysis
<b>CDKN1A-interacting zinc finger protein 1 is a novel biomarker for lung squamous cell carcinoma (Zhou X, et al., 2018).</b>	- CIZ1 overexpression in nucleus and cytoplasm	- IC in tissue microarrays (TMAs) -Western blot -IF
<b>CIZ1 interacts with YAP and activates its transcriptional activity in hepatocellular carcinoma cells (Lei L, et al., 2016).</b>	-CIZ1 interacted with YAP in HCC cells via AD and promotes its activity - Knocking down the expression of CIZ1 abolished the promoting effects of YAP on the growth of HCC cells.	-GST pull-down assay - Luciferase expression assay -ChIP - Crystal violet and Boyden chamber assays.
<b>The Role of Cdkn1A-Interacting Zinc Finger Protein 1 (CIZ1) in DNA Replication and Pathophysiology (Liu Q, et al., 2016).</b>	-Summary of CIZ1 alternative splicing and biologically relevant CIZ1 interacting proteins.	- Bibliographic review

<b>CIZ1 is upregulated in hepatocellular carcinoma and promotes the growth and migration of the cancer cells (Wu J, et al., 2016).</b>	<ul style="list-style-type: none"> <li>-CIZ1 is upregulated in hepatocellular carcinoma clinical samples and cell lines</li> <li>-Overexpression of CIZ1 promotes the growth and migration of the HCC cells</li> <li>- CIZ1 Knocking down reduced the metastasis of HepG2 cells in vivo</li> </ul>	<ul style="list-style-type: none"> <li>-qPCR</li> <li>- Luciferase expression assay</li> <li>- Crystal violet and Boyden chamber assays.</li> <li>-Metastasis assay</li> </ul>
<b>CIZ1 is upregulated in hepatocellular carcinoma and promotes the growth and migration of the cancer cells (Wu J, et al., 2016).</b>	<ul style="list-style-type: none"> <li>CIZ1 is upregulated in hepatocellular carcinoma clinical samples and cell lines.</li> <li>-CIZ1 promotes growth and migration of the HCC cell.</li> <li>-CIZ1 activates the transcriptional activity of YAP in HCC cells.</li> <li>- Knocking down the expression of CIZ1 inhibited the metastasis of HepG2 cells in vivo.</li> </ul>	<ul style="list-style-type: none"> <li>-Western blot</li> <li>-qPCR</li> <li>-Cell proliferation and colony formation assays</li> <li>- IC</li> </ul>
<b>Ciz1 promotes tumorigenicity of prostate carcinoma cells (Liu T, et al., 2015).</b>	<ul style="list-style-type: none"> <li>-Elevated CIZ1 expression in prostatic carcinoma tissues and cell lines.</li> <li>-CIZ1 gene silencing decreased: <ul style="list-style-type: none"> <li>-Prostate carcinoma cells capacity for proliferation and colony formation.</li> <li>- Tumour formation in number and size in nude mice.</li> <li>- Prostate cancer-related gene expression in PC-3 cells</li> </ul> </li> </ul>	<ul style="list-style-type: none"> <li>-Western Blot</li> <li>-qPCR</li> <li>-Cell proliferation and colony formation assays</li> <li>- IC</li> </ul>
<b>CIZ1 promoted the growth and migration of gallbladder cancer cells (Zhang D et al., 2015).</b>	<ul style="list-style-type: none"> <li>-CIZ1 was upregulated in gallbladder cancer tissues.</li> <li>-Forced expression of CIZ1 promoted the growth and migration of gallbladder cancer cells.</li> <li>-Downregulation of CIZ1 inhibited the growth and migration of gallbladder cancer cells.</li> <li>-CIZ1 positively regulated beta-catenin/TCF4 signalling.</li> <li>-Knocking down the expression of CIZ1 impaired the tumorigenicity of SGC-996 cells in vivo.</li> </ul>	<ul style="list-style-type: none"> <li>-Western blot</li> <li>-Cell proliferation and colony formation assays</li> <li>- IC</li> <li>- Crystal violet and Boyden chamber assays</li> <li>-qPCR</li> </ul>
<b>Ciz1 is a novel predictor of survival in human colon cancer (Wang DQ, et al., 2014).</b>	<ul style="list-style-type: none"> <li>- Upregulation of Ciz1 mRNA expression in both poorly and well differentiated colon cancer tissue.</li> <li>-Association between Ciz1 expression and colon cancer patient survival.</li> </ul>	<ul style="list-style-type: none"> <li>-qPCR</li> <li>- IC</li> <li>-hCIZ1 ELISA</li> </ul>
<b>CIZ1 regulates the proliferation, cycle distribution and colony formation of RKO human colorectal cancer cells (Yin J, et al., 2013).</b>	<ul style="list-style-type: none"> <li>-CIZ1 was highly expressed in RKO CRC cells</li> <li>- CIZ1 knockdown inhibits cell proliferation, colony formation, induces cell cycle arrest and increases apoptosis of RKO cells.</li> <li>-The percentage of G0/G1 stage cells was increased in the CIZ1-siRNA group while the percentage of cells in the S phase was decreased.</li> </ul>	<ul style="list-style-type: none"> <li>-qPCR</li> <li>-Western Blot</li> <li>-Flow cytometry</li> <li>-IF</li> </ul>

<b>Variant Ciz1 is a circulating biomarker for early-stage lung cancer (Higgins G, et al., 2012)</b>	<ul style="list-style-type: none"> <li>-CIZ1b variant is a lung-specific biomarker detectable in 1ul of plasma</li> <li>-At least 40-fold elevation in bulk tumour RNA from neuroendocrine tumours.</li> <li>-b-variant shRNA restrained cell proliferation in culture and xenograft tumour growth.</li> </ul>	<ul style="list-style-type: none"> <li>-qPCR</li> <li>- IC</li> <li>-Western Blot</li> </ul>
<b>Differential detection of alternatively spliced variants of Ciz1 in normal and cancer cells using a custom exon-junction microarray (Rahman FA, al., 2010).</b>	<ul style="list-style-type: none"> <li>-Expression of alternative exon 1s, being 1c the most represented.</li> <li>-A cancer-associated variant, with partial deletion of exon 8 and 12 and skipping of exon 9, 10 and 11 (CIZ1F)</li> </ul>	<ul style="list-style-type: none"> <li>-qPCR</li> <li>-Exon-Junction Microarray.</li> </ul>
<b>Identification of multi-SH3 domain-containing protein interactome in pancreatic cancer: a yeast two-hybrid approach (Thalappilly S, al., 2008).</b>	<ul style="list-style-type: none"> <li>-CIZ1 interacts with multi SH3 domains proteins overexpressed in pancreatic cancer.</li> <li>-Interaction of CIZ1 with the cytoplasmatic scaffold protein SH3BP4 facilitates led to modulation of cell cycle progression and proliferation.</li> </ul>	<ul style="list-style-type: none"> <li>-Microarray</li> <li>-Western blot</li> <li>-Two hybrid system</li> </ul>
<b>Altered splicing in exon 8 of the DNA replication factor CIZ1 affects subnuclear distribution and is associated with Alzheimer's disease (Dahmcke CM, et al., 2008).</b>	<ul style="list-style-type: none"> <li>-Splice variant CIZ1S, which contains a 168 nt deletion in exon 8, is upregulated in AD.</li> <li>-Levels of the full-length CIZ1 are unaltered in AD, whereas expression of the splice variant CIZ1S is upregulated 2.5-fold.</li> <li>-Association of CIZ1 with the nuclear matrix requires a glutamine-rich domain.</li> </ul>	<ul style="list-style-type: none"> <li>-qPCR</li> <li>-IC</li> <li>-Western blot</li> </ul>
<b>Cancer-associated missplicing of exon 4 influences the subnuclear distribution of the DNA replication factor CIZ1 (Rahman F et al., 2007).</b>	<ul style="list-style-type: none"> <li>-At least four exons (2, 4, 6, and 8) appear to be alternatively spliced.</li> <li>-Exon 4 skipping is common in the ET-derived cell lines.</li> <li>-Observations suggest that exclusion of Ciz1 exon 4 is a physiologically relevant event that may be subject to regulation in normal cells.</li> <li>-Mononucleotide T repeat length influences skipping of CIZ1 exon 4</li> <li>-Amplification of the CIZ1 locus in some cancer cells.</li> <li>-CIZ1 ΔE4 is active in DNA replication but fails to form foci.</li> </ul>	<ul style="list-style-type: none"> <li>-qPCR</li> <li>-Exon trap assay</li> <li>-Cell-free replication assay</li> <li>-IF</li> </ul>
<b>CIZ1, a Novel DNA-binding coactivator of the estrogen receptor alpha, confers hypersensitivity to estrogen action (den Hollander P, et al., 2006).</b>	<ul style="list-style-type: none"> <li>-CIZ1 is an estrogen-inducible gene.</li> <li>-CIZ1 is a coactivator of ER-alpha</li> <li>-CIZ1 promotes tumorigenic phenotypes in breast cancer cells</li> </ul>	<ul style="list-style-type: none"> <li>-qPCR</li> <li>-Soft agar colony assay</li> <li>-Western, ChIP</li> <li>-GST-pull off</li> <li>-IC, IF</li> </ul>
<b>Ciz1, Cip1 interacting zinc finger protein 1 binds the consensus DNA sequence ARYSR(0-2)YYAC (Warder DE, Keherly MJ, 2003).</b>	<ul style="list-style-type: none"> <li>-CIZ1 is localised to the nucleus and is expressed in a variety of tissues.</li> </ul>	<ul style="list-style-type: none"> <li>-Northern blot</li> <li>-Western blot</li> <li>-PCR</li> <li>-IF</li> </ul>

ChIP: Chromatin immunoprecipitation, qPCR: qRT-PCR, IF: Immunofluorescence analysis;

IC: Immunohistochemical analysis

## 2. Negative control of serial nuclear extraction.

To verify the specificity of the signal detected in immunofluorescence analyses after the different extraction steps, a set of MDA-MB-231 cells were subjected to a full serial nuclear extraction whereas instead of primary antibody, cells were incubated with a mock buffer. Then the cells were incubated with the same secondary antibodies previously utilised for detecting anti-CIZ1-AD and anti-CIZ1-RD antibodies. From that point, cells were treated following standard serial nuclear extraction protocol as described in Chapter 2. After each extraction step, practically undetectable levels of unspecific binding were observed (Fig. A.1), discarding the possibility that this unspecific signal could account for part of the signal detected after any of the extraction steps of the serial nuclear matrix extraction analyses.

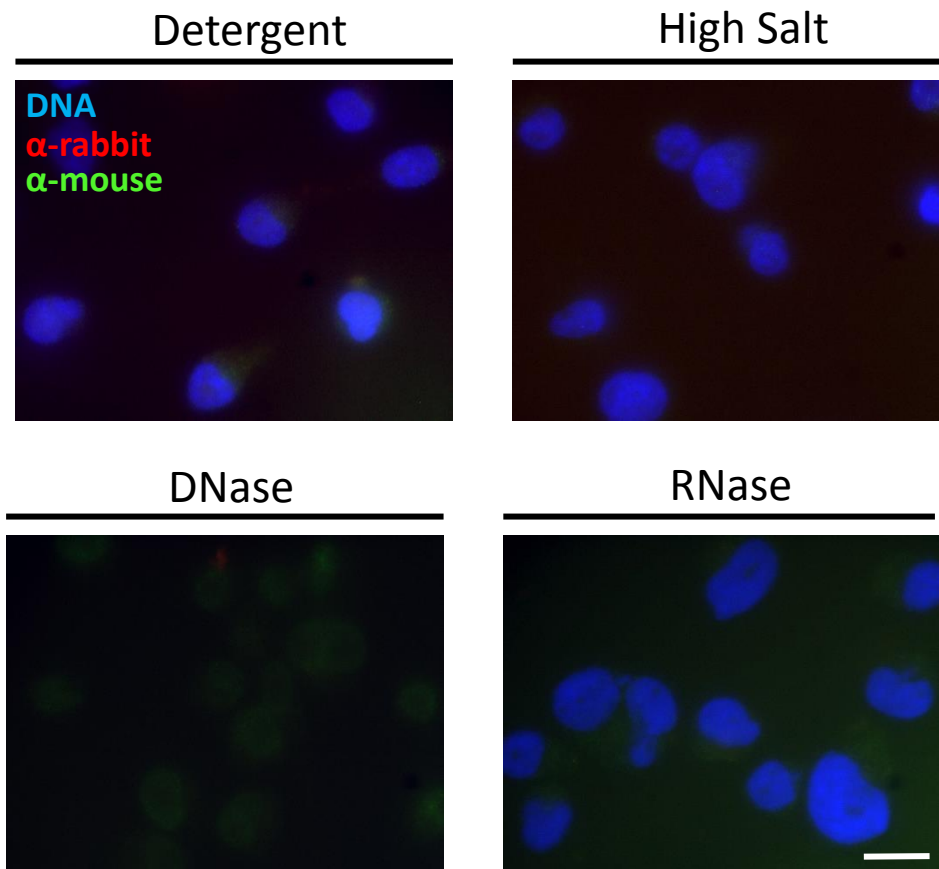


**Figure A.1. Negative control of serial nuclear extraction.** Pictures were taken with the same parameters and edition utilised for the nuclear matrix extraction analyses (Chapter 5, Fig. 5.2). Scale bar represents 10 microns.

### 3. Antibody validation.

In order to validate the specificity of the unpublished CIZ1 antibodies utilised in this study, comparative CIZ1 immunodetection analyses were performed in detergent-treated 1-7 HB2 cells (Fig. A.2A). Both the commercial anti-CIZ1-AD antibody ‘Nov4’<sup>57</sup> (known to recognise human and mouse CIZ1, utilised for western blot analyses in this study) and the unpublished anti-CIZ1-AD antibody ‘87’ (utilised in immunofluorescence analyses in this study) can detect CIZ1 foci and also aggregates at Xi, suggesting that ‘87’ is a suitable tool for immunodetection of CIZ1-AD. Moreover, this antibody has been successfully mapped using synthetic CIZ1 peptides (L. Williamson unpublished).

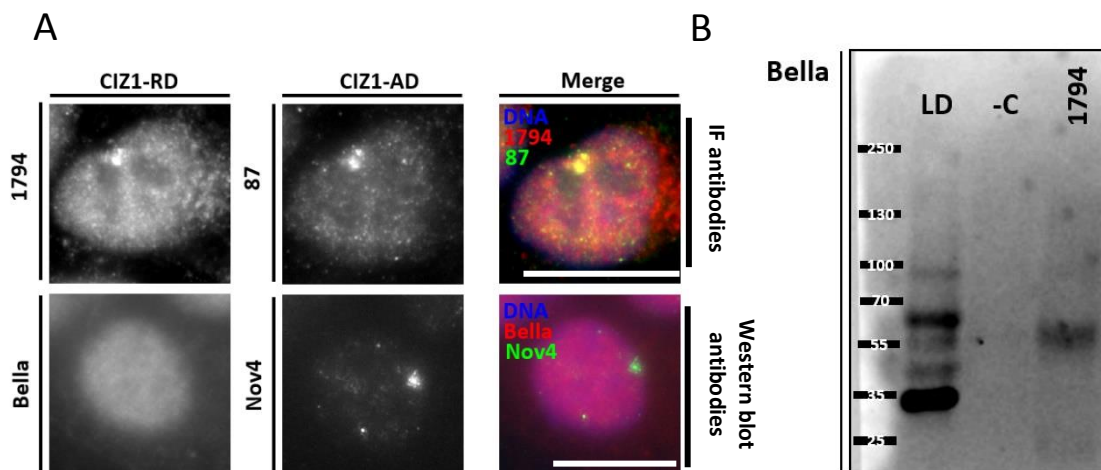


**Figure A.2. Immunofluorescence-Western blot antibody validation.** A) Comparative immunodetection of CIZ1 by different antibodies. B) Immunoprecipitated CIZ1 using 1794 antibody detected by western blot using Bella antibody. LD: Loading control. -C: negative control (no antibody added when immunoprecipitating). Scale bars represent 10 microns.

In contrast, unlike the anti-CIZ1-RD rabbit polyclonal antibody ‘1794’ (validated in previous publications<sup>7</sup>), which could detect CIZ1 at Xi, the unpublished anti-CIZ1-RD monoclonal antibody ‘Bella’ (utilised for western blotting in this study) did not immunodetect CIZ1 at Xi and provided a very diffuse signal (Fig. A.2A). This significant difference in signal localisation and intensity raised concerns about the specificity of Bella antibody. To clarify this, a preliminary immunoprecipitation assay using ‘1794’ to capture native CIZ1-RD-containing proteins from

normal breast cell (1-7HB2) lysates was performed. The precipitated proteins were then analysed by western blot, using 'Bella' antibody (Fig. A.2B). An approximately 60KDa CIZ1 form captured by '1794' was detectable by 'Bella', representing a first evidence of reactivity with the same entity. It is important to note as a limitation for this experiment that '1794' antibody specificity was validated using murine CIZ1 peptides. In any case, further verification of the specificity of CIZ1 antibodies in HPMECs and cell lines utilised in this study using different experimental approaches, as well as the inclusion of an isotype control in the immunoprecipitation reaction are essential for the faithful interpretation of the CIZ1 protein analysis performed in this study.

## References

---

1. Bebenek, K. & Kunkel, T. A. Functions of DNA Polymerases. in *Advances in protein chemistry* **69**, 137–165 (2004).
2. Barnum, K. J. & O'Connell, M. J. Cell cycle regulation by checkpoints. *Methods Mol. Biol.* **1170**, 29–40 (2014).
3. Lim, S. & Kaldis, P. Cdks, cyclins and CKIs: roles beyond cell cycle regulation. *Development* **140**, 3079–93 (2013).
4. Lukin, D. J., Carvajal, L. A., Liu, W., Resnick-Silverman, L. & Manfredi, J. J. p53 Promotes cell survival due to the reversibility of its cell-cycle checkpoints. *Mol. Cancer Res.* **13**, 16–28 (2015).
5. Mitsui, K., Matsumoto, A., Ohtsuka, S., Ohtsubo, M. & Yoshimura, A. Cloning and Characterization of a Novel p21 Cip1/Waf1-Interacting Zinc Finger Protein, Ciz1. (1999).
6. Ainscough, J. F.-X. *et al.* C-terminal domains deliver the DNA replication factor Ciz1 to the nuclear matrix. *J. Cell Sci.* **120**, 115–124 (2006).
7. Coverley, D., Marr, J. & Ainscough, J. Ciz1 promotes mammalian DNA replication. *J. Cell Sci.* **118**, 101–12 (2005).
8. Ainscough, J. F.-X. *et al.* C-terminal domains deliver the DNA replication factor Ciz1 to the nuclear matrix. *J. Cell Sci.* **120**, 115–24 (2007).
9. Dalton, S. Cell cycle control of chromosomal DNA replication. *Immunol. Cell Biol.* **76**, 467–472 (1998).
10. Mehanna, A. & Diffley, J. F. X. Pre-replicative complex assembly with purified proteins. *Methods* **57**, 222–226 (2012).
11. Duzdevich, D. *et al.* The dynamics of eukaryotic replication initiation: Origin specificity, licensing, and firing at the single-molecule level. *Mol. Cell* (2015). doi:10.1016/j.molcel.2015.03.017
12. Fragkos, M., Ganier, O., Coulombe, P. & Méchali, M. DNA replication origin activation in space and time. *Nature Reviews Molecular Cell Biology* (2015). doi:10.1038/nrm4002
13. Pauzaitė, T., Thacker, U., Tollitt, J. & Copeland, N. A. Emerging roles for ciz1 in cell cycle regulation and as a driver of tumorigenesis. *Biomolecules* (2017). doi:10.3390/biom7010001
14. Heller, R. C. *et al.* Eukaryotic Origin-Dependent DNA Replication In Vitro Reveals Sequential Action of DDK and S-CDK Kinases. *Cell* **146**, 80–91 (2011).
15. Perez-Arnaiz, P., Bruck, I. & Kaplan, D. L. Mcm10 coordinates the timely assembly and activation of the replication fork helicase. *Nucleic Acids Res.* **44**, 315–329 (2016).
16. Yeeles, J. T. P., Deegan, T. D., Janska, A., Early, A. & Diffley, J. F. X. Regulated eukaryotic DNA replication origin firing with purified proteins. *Nature* **519**, 431–435 (2015).
17. Onesti, S. & MacNeill, S. A. Structure and evolutionary origins of the CMG complex. *Chromosoma* **122**, 47–53 (2013).
18. Sun, J. *et al.* The architecture of a eukaryotic replisome. *Nat. Struct. Mol. Biol.* **22**, 976–

- 982 (2015).
19. Sengupta, S., van Deursen, F., de Piccoli, G. & Labib, K. Dpb2 integrates the leading-strand DNA polymerase into the eukaryotic replisome. *Curr. Biol.* **23**, 543–52 (2013).
  20. Copeland, N. A., Sercombe, H. E., Ainscough, J. F. X. & Coverley, D. Ciz1 cooperates with cyclin-A-CDK2 to activate mammalian DNA replication in vitro. *J. Cell Sci.* **123**, 1108–15 (2010).
  21. Coverley, D., Marr, J. & Ainscough, J. Ciz1 promotes mammalian DNA replication. *J. Cell Sci.* (2005). doi:10.1242/jcs.01599
  22. Den Hollander, P., Rayala, S. K., Coverley, D. & Kumar, R. Ciz1, a novel DNA-binding coactivator of the estrogen receptor  $\alpha$ , confers hypersensitivity to estrogen action. *Cancer Res.* (2006). doi:10.1158/0008-5472.CAN-06-2336
  23. den Hollander, P. & Kumar, R. Dynein Light Chain 1 Contributes to Cell Cycle Progression by Increasing Cyclin-Dependent Kinase 2 Activity in Estrogen-Stimulated Cells. *Cancer Res.* **66**, 5941–5949 (2006).
  24. Rahman, F. A., Aziz, N. & Coverley, D. Differential detection of alternatively spliced variants of Ciz1 in normal and cancer cells using a custom exon-junction microarray. *BMC Cancer* **10**, 1–12 (2010).
  25. Heard, E. & Disteché, C. M. Dosage compensation in mammals: Fine-tuning the expression of the X chromosome. *Genes and Development* **20**, 1848–1867 (2006).
  26. Cerase, A. *et al.* Spatial separation of Xist RNA and polycomb proteins revealed by superresolution microscopy. *Proc. Natl. Acad. Sci. U. S. A.* **111**, 2235–40 (2014).
  27. Heard, E. *et al.* Methylation of histone H3 at Lys-9 is an early mark on the X chromosome during X inactivation. *Cell* **107**, 727–38 (2001).
  28. Pollex, T. & Heard, E. Recent advances in X-chromosome inactivation research. *Curr. Opin. Cell Biol.* **24**, 825–32 (2012).
  29. Heard, E. Dosage compensation in mammals: fine-tuning the expression of the X chromosome. *Genes Dev.* **20**, 1848–1867 (2006).
  30. Ridings-Figueroa, R. *et al.* The nuclear matrix protein CIZ1 facilitates localization of Xist RNA to the inactive X-chromosome territory. *Genes Dev.* **31**, 876–888 (2017).
  31. Stewart, E. R. *et al.* Maintenance of epigenetic landscape requires CIZ1 and is corrupted in differentiated fibroblasts in long-term culture. *Nat. Commun.* **10**, 460 (2019).
  32. Warder, D. E. & Keherly, M. J. Ciz1, Cip1 interacting zinc finger protein 1 binds the consensus DNA sequence ARYSR(0-2)YYAC. *J. Biomed. Sci.* **10**, 406–417 (2003).
  33. Hammer, M. *et al.* Blepharospasm: A genetic screening study in 132 patients. *Park. Relat. Disord.* (2019). doi:10.1016/j.parkreldis.2019.04.003
  34. Xiao, J. *et al.* Mutations in CIZ1 cause adult-onset primary cervical dystonia. *Ann. Neurol.* **71**, 458 (2012).
  35. Dahmcke, C. M., Büchmann-Møller, S., Jensen, N. A. & Mitchelmore, C. Altered splicing in exon 8 of the DNA replication factor CIZ1 affects subnuclear distribution and is associated with Alzheimer’s disease. *Mol. Cell. Neurosci.* **38**, 589–594 (2008).
  36. Higgins, G. *et al.* Variant Ciz1 is a circulating biomarker for early-stage lung cancer. *Proc.*

*Natl. Acad. Sci.* (2012). doi:10.1073/pnas.1210107109

37. Coverley, D. *et al.* A quantitative immunoassay for lung cancer biomarker CIZ1b in patient plasma. *Clin. Biochem.* **50**, 336–343 (2017).
38. Den Hollander, P., Rayala, S. K., Coverley, D. & Kumar, R. Ciz1, a novel DNA-binding coactivator of the estrogen receptor  $\alpha$ , confers hypersensitivity to estrogen action. *Cancer Res.* **66**, 11021–11029 (2006).
39. Yin, J. *et al.* CIZ1 regulates the proliferation, cycle distribution and colony formation of RKO human colorectal cancer cells. *Mol. Med. Rep.* **8**, 1630–1634 (2013).
40. Wang, D. qing *et al.* Ciz1 is a novel predictor of survival in human colon cancer. *Exp. Biol. Med.* **239**, 862–870 (2014).
41. Liu, T. *et al.* *Ciz1 promotes tumorigenicity of prostate carcinoma cell.* (1996).
42. Wu, J., Lei, L., Gu, D., Liu, H. & Wang, S. CIZ1 is upregulated in hepatocellular carcinoma and promotes the growth and migration of the cancer cells. *Tumor Biol.* **37**, 4735–4742 (2016).
43. Lei, L., Wu, J., Gu, D., Liu, H. & Wang, S. CIZ1 interacts with YAP and activates its transcriptional activity in hepatocellular carcinoma cells. *Tumor Biol.* (2016). doi:10.1007/s13277-016-4866-8
44. Chen, X. *et al.* CIZ1 knockdown suppresses the proliferation of bladder cancer cells by inducing apoptosis. *Gene* 143946 (2019). doi:10.1016/j.gene.2019.143946
45. Zhang, D. *et al.* CIZ1 promoted the growth and migration of gallbladder cancer cells. *Tumor Biol.* **36**, 2583–2591 (2015).
46. Wang, Y. *et al.* CIZ1 Expression Is Upregulated in Hemangioma of the Tongue. *Pathol. Oncol. Res.* (2018). doi:10.1007/s12253-018-0495-4
47. Chaligné, R. *et al.* The inactive X chromosome is epigenetically unstable and transcriptionally labile in breast cancer. *Genome Res.* **25**, 488–503 (2015).
48. O'Donovan, P. J. & Livingston, D. M. BRCA1 and BRCA2: breast/ovarian cancer susceptibility gene products and participants in DNA double-strand break repair. *Carcinogenesis* **31**, 961–967 (2010).
49. Chaligné, R. & Heard, E. X-chromosome inactivation in development and cancer. *FEBS Lett.* **588**, 2514–2522 (2014).
50. Bartek, J. *et al.* Efficient immortalization of luminal epithelial cells from human mammary gland by introduction of simian virus 40 large tumor antigen with a recombinant retrovirus. *Proc. Natl. Acad. Sci. U. S. A.* **88**, 3520–4 (1991).
51. Rahman, F. A., Ainscough, J. F. X., Copeland, N. & Coverley, D. Cancer-associated missplicing of exon 4 influences the subnuclear distribution of the DNA replication factor CIZ1. *Hum. Mutat.* **28**, 993–1004 (2007).
52. Swarts, D. R. A., Stewart, E. R., Higgins, G. S. & Coverley, D. CIZ1-F, an alternatively spliced variant of the DNA replication protein CIZ1 with distinct expression and localisation, is overrepresented in early stage common solid tumours. *Cell Cycle* **17**, 2268–2283 (2018).
53. Stewart, E. R. & Coverley, D. Visualization of Hidden Epitopes at the Inactive X Chromosome. in 103–112 (Humana, New York, NY, 2018). doi:10.1007/978-1-4939-

54. Livak, K. J. & Schmittgen, T. D. Analysis of Relative Gene Expression Data Using Real-Time Quantitative PCR and the  $2^{-\Delta\Delta CT}$  Method. *Methods* **25**, 402–408 (2001).
55. Copeland, N. A., Sercombe, H. E., Ainscough, J. F. X. & Coverley, D. Ciz1 cooperates with cyclin-A-CDK2 to activate mammalian DNA replication in vitro. *J. Cell Sci.* (2010). doi:10.1242/jcs.059345
56. Ainscough, J. F.-X. *et al.* C-terminal domains deliver the DNA replication factor Ciz1 to the nuclear matrix. *J. Cell Sci.* (2006). doi:10.1242/jcs.03327
57. Ridings-Figueroa, R. *et al.* The nuclear matrix protein CIZ1 facilitates localization of Xist RNA to the inactive X-chromosome territory. *Genes Dev.* **31**, 876–888 (2017).
58. Zhou, X., Liu, Q., Wada, Y., Liao, L. & Liu, J. CDKN1A-interacting zinc finger protein 1 is a novel biomarker for lung squamous cell carcinoma. *Oncol. Lett.* **15**, 183–188 (2018).
59. Lei, L., Wu, J., Gu, D., Liu, H. & Wang, S. CIZ1 interacts with YAP and activates its transcriptional activity in hepatocellular carcinoma cells. *Tumor Biol.* **37**, 11073–11079 (2016).
60. Greaves, E. A., Copeland, N. A., Coverley, D. & Ainscough, J. F. X. Cancer-associated variant expression and interaction of CIZ1 with cyclin A1 in differentiating male germ cells. *J. Cell Sci.* (2012). doi:10.1242/jcs.101097
61. Riaz, M. *et al.* miRNA expression profiling of 51 human breast cancer cell lines reveals subtype and driver mutation-specific miRNAs. *Breast Cancer Res.* **15**, R33 (2013).
62. Dai, X., Cheng, H., Bai, Z. & Li, J. Breast cancer cell line classification and its relevance with breast tumor subtyping. *Journal of Cancer* **8**, 3131–3141 (2017).
63. Qu, Y. *et al.* Evaluation of MCF10A as a Reliable Model for Normal Human Mammary Epithelial Cells. *PLoS One* **10**, e0131285 (2015).
64. Dubois, M.-L. & Boisvert, F.-M. The Nucleolus: Structure and Function. in *The Functional Nucleus* 29–49 (Springer International Publishing, 2016). doi:10.1007/978-3-319-38882-3\_2
65. Colognori, D., Sunwoo, H., Kriz, A. J., Wang, C.-Y. & Lee, J. T. Xist Deletional Analysis Reveals an Interdependency between Xist RNA and Polycomb Complexes for Spreading along the Inactive X. *Mol. Cell* **74**, 101–117.e10 (2019).
66. Fox, A. H., Nakagawa, S., Hirose, T. & Bond, C. S. Paraspeckles: Where Long Noncoding RNA Meets Phase Separation. *Trends Biochem. Sci.* **43**, 124–135 (2018).
67. Shin, Y. & Brangwynne, C. P. Liquid phase condensation in cell physiology and disease. *Science* **357**, eaaf4382 (2017).
68. Smeets, D. *et al.* Three-dimensional super-resolution microscopy of the inactive X chromosome territory reveals a collapse of its active nuclear compartment harboring distinct Xist RNA foci. *Epigenetics Chromatin* **7**, 8 (2014).
69. Cerase, A. *et al.* Phase separation drives X-chromosome inactivation: a hypothesis. *Nature Structural and Molecular Biology* **26**, 331–334 (2019).
70. Cerase, A., Pintacuda, G., Tattermusch, A. & Avner, P. Xist localization and function: new insights from multiple levels. *Genome Biol.* **16**, 166 (2015).

71. Pintacuda, G. *et al.* hnRNPK Recruits PCGF3/5-PRC1 to the Xist RNA B-Repeat to Establish Polycomb-Mediated Chromosomal Silencing. *Mol. Cell* **68**, 955-969.e10 (2017).
72. Liu, Q., Niu, N., Wada, Y. & Liu, J. The role of Cdkn1A-interacting zinc finger protein 1 (CIZ1) in DNA replication and pathophysiology. *Int. J. Mol. Sci.* **17**, 1–12 (2016).
73. Sirchia, S. M. *et al.* Misbehaviour of XIST RNA in breast cancer cells. *PLoS One* **4**, e5559 (2009).
74. Sivaganesan, M., Haugland, R. A., Chern, E. C. & Shanks, O. C. Improved strategies and optimization of calibration models for real-time PCR absolute quantification. *Water Res.* **44**, 4726–4735 (2010).
75. Di Fede, G. *et al.* A recessive mutation in the APP gene with dominant-negative effect on amyloidogenesis. *Science* **323**, 1473–7 (2009).
76. Silva, J. L., Rangel, L. P., Costa, D. C. F., Cordeiro, Y. & Gallo, C. V. D. M. Expanding the prion concept to cancer biology: dominant-negative effect of aggregates of mutant p53 tumour suppressor. *Biosci. Rep.* **33**, (2013).